generate HDL may be the cause of altered cholesterol metabolism in an Alzheimer's disease (AD) brain (Demeester et al., 2000; Molander-Melin et al., 2005) and may explain how ApoE4 serves as a strong risk factor for AD development (Corder et al., 1993; Strittmatter et al., 1993). However, the molecular mechanism underlying ApoE-isoform-dependent HDL generation remains to be elucidated.

The ApoE molecule has two distinct domains, namely, the 22-kDa amino-terminal (residues 1–191) and 10-kDa carboxyl-terminal domains (residue 218–299), that unfold independently of each other (Wetterau et al., 1988; Morrow et al., 2000). It has been demonstrated that ApoE4 amino- and carboxyl-domain interaction is responsible for the ApoE-isoform dependent association with lipid particles (Weisgraber, 1990; Dong and Weisgraber, 1996; Saito et al., 2003). The domain interaction in ApoE4 under physiological conditions has also been confirmed at the cellular level (Xu et al., 2004) and in vivo (Raffai et al., 2001; Ramaswamy et al., 2005), suggesting that the presence or absence of the domain interaction can explain ApoE-isoform dependent lipid efflux. In addition, there are ApoE-isoform dependent differences in the structure and stability of the 22-kDa amino-terminal fragment (22-kDa-ApoE), which affect their binding affinities to lipids (Morrow et al., 2000, 2002; Segall et al., 2002; Hatters et al., 2005), suggesting that the 22-kDa-ApoE that lacks the domain interaction may also explain an isoform-dependent lipid efflux.

In this study, we investigated the molecular mechanisms, by which intact ApoE3 has a greater ability to induce cholesterol efflux than intact-ApoE4 by using cultured rat neurons and astrocytes prepared from ApoE knockout mouse brain to exclude the effect of endogenously generated and secreted ApoE. We found that the intramolecular amino- and carboxyl-terminal domain interaction is partially responsible for this ApoE-isoform dependency. To our surprise, 22-kDa-ApoE3 has a greater ability to induce cholesterol efflux than 22-kDa-ApoE4. This is because 22-kDa-ApoE3 forms dimers, whereas 22-kDa-ApoE4 does not. These findings suggest that cholesterol efflux induced by ApoE is regulated by two major factors: the presence or absence of intermolecular dimer formation and the intramolecular domain interaction.

EXPERIMENTAL PROCEDURES

Cell Culture

All experiments were performed in compliance with existing laws and institutional guidelines. Neuron-rich cultures were prepared from rat cerebral cortices as previously described (Michikawa et al., 2001). Cerebral cortices from rat brains were dissected, freed of meninges, and diced into small fragments. Cortical fragments were incubated in 2.5% trypsin and 2 mg/ml DNase I in phosphate-buffered saline (PBS) (8.1 mM Na_2HPO_4, 1.5 mM KH_2PO_4, 137 mM NaCl, and 2.7 mM KCl; pH 7.4) at 37°C for 15 min. The fragments were then dissociated into single cells by pipetting. The dissociated cells were suspended in a feeding medium and plated onto poly-D-lysine-coated 12-well plates at a cell density of 1×10^6/ml in Dulbecco modified Eagle's medium nutrient mixture (DMEM/F-12; 50:50%) containing N_2 supplements plus 7.5% bovine albumin fraction V.

Highly astrocyte-rich cultures were prepared according to a previously described method (Michikawa et al., 2001). In brief, brains of postnatal day 2 ApoE knockout mice were removed under anesthesia. The cerebral cortices from the mouse brains were dissected, freed of meninges, and diced into small fragments. Cortical fragments were incubated in 0.25% trypsin and 2 mg/ml DNase I in PBS (8.1 mM Na_2HPO_4, 1.5 mM KH_2PO_4, 137 mM NaCl and 2.7 mM KCl; pH 7.4) at 37°C for 15 min. The fragments were then dissociated into single cells by pipetting. The dissociated cells were seeded in 75-cm^2 dishes at a cell density of 1×10^7 in DMEM nutrient mixture containing 10% FBS and 1% penicillin/streptomycin solution (Invitrogen Corporation, Carlsbad, CA). After 10 days of incubation in vitro, astrocytes in the monolayer were trypsinized (0.1%) and reseeded onto twelve-well dishes. The astrocyte-rich cultures were maintained in DMEM containing 10% FBS until use.

ApoE Preparation

The full-length human ApoE3 and ApoE4 and their 22- and 10-kDa fragments were expressed and purified as described (Saito et al., 2001). The cDNA for full-length human ApoE3 and ApoE4, the 22-kDa fragments, or the 10-kDa fragment were ligated into a thioredoxin fusion expression vector pET32a and transformed into the *Escherichia coli* strain BL21 star (DE3). The transformed *E. coli* were cultured in LB medium at 37°C, and thioredoxin-ApoE expression was induced with isopropyl-β-D-galactopyranoside for 3 hr. After the bacterial pellet was sonicated and the lysate was centrifuged to remove debris, the fusion protein was cleaved with thrombin to remove thioredoxin from full-length ApoE3, ApoE4 or the 22- or 10-kDa fragment. For the full-length ApoE3 and ApoE4, the fusion protein was complexed with DMPC before it was cleaved with thrombin to protect the protease susceptible internal hinge region. After inactivation of the thrombin with β-mercaptoethanol, the mixture was lyophilized and delipidated, and the ApoE pellet was dissolved in 6 M guanidine–HCl, pH 7.4, containing 1% β-mercaptoethanol. The ApoE was isolated by gel filtration chromatography on a Sephacryl S-300 column. For further purification (>95%), the proteins were subjected to gel filtration with a Superdex 75 column or anion exchange chromatography with a HiTrap Q column

When we used ApoE and ApoE fragments, the recombinant ApoEs were dissolved in 5 M guanidine–HCl. The resulting solutions were dialyzed against PBS at 4°C for 16 hr. Each ApoE level was determined with a BCA protein assay kit (Pierce, Rockford, IL).

Determination of Levels of Cholesterol and Phosphatidylcholine (PC) Released From Neurons and Astrocytes Labeled With [^{14}C]acetate

Astrocytes plated in twelve-well dishes were cultured in DMEM containing 10% FBS and 1% penicillin/streptomycin

solution for 72 hr. The cultures were then treated with 37 kBq/ml [^{14}C]acetate (Moravek Biochemicals Inc., Brea, CA) for 48 hr. The astrocytes were washed in DMEM two times and treated with 0.3 μM ApoE in DMEM for 24 hr. To analyze dose-dependent effects, the astrocytes were treated with 0.03 μM, 0.1 μM, 0.3 μM and 1.0 μM ApoE; to analyze time-dependent effects, the astrocytes were treated and maintained for 8, 24 and 48 hr. The culture medium was quickly removed and the astrocytes were dried at room temperature. 1.0 ml of the conditioned culture medium was extracted with 4.0 ml of hexane/isopropyl alcohol (3:2 v/v). For the extraction of intracellular lipids, dried astrocytes were incubated in hexane/isopropyl alcohol (3:2 v/v) for 1 hr at room temperature. The solvent from each plate was removed and dried under N_2 gas. The organic phase was redissolved in 200 μl of hexane/isopropyl alcohol (3:2 v/v), and 10 μl of each sample was spotted on activated-silica-gel high- performance thin layer chromatography plates (Merck); the lipids were separated by sequential one-dimensional chromatography by using chloroform/methanol/acetic acid/water (25:15:4:2, v/v), followed by another run in hexane/diethyl ether/acetic acid (80:30:1). [^{14}C]Cholesterol and [^{14}C]PC were used as standards. The chromatography plates were exposed to radiosensitive films, and each lipid was visualized and quantified with BAS2500 (Fuji Film, Tokyo, Japan). The levels of [^{14}C]cholesterol and [^{14}C]PC efflux were calculated by the following formula: % efflux = media × 100/(media + cell).

Dimerization of 22-kDa-ApoE3

The pure 22-kD-ApoE3 was obtained by reduction with 10 mM dithiothreitol (DTT) in 5 M guanidine–HCl buffer. The dimer was formed by incubation of the monomer in oxygenated 5 M guanidine–HCl at 10 mg/ml for 2 weeks at 4°C. Residual monomer was removed by passage of the protein solution through a thiopropyl Sepharose 6B column (GE Healthcare, Piscataway, NJ) according to the manufacturer's instructions.

Dimerization of Intact ApoE3

The ApoE3 (1 mg/ml in 6 M urea, and 10 mM Tris-HCl) used was a mixture of monomeric and dimeric ApoEs. The mixture was reduced to generate monomeric ApoE3 by adding 10 mM DTT, incubated at 4°C for 16 hr, dialyzed against 6 M urea in 10 mM Tris-HCl solution, and oxidized by stirring at 4°C for 3 days. Then it was loaded onto a 2-ml-bed-volume prepacked 6% cross-linked beaded agarose gel column with a SulfoLink kit (Pierce, Rockford, IL) and equilibrated with PBS. Dimeric ApoE3 was eluted with PBS.

Western Blot Analysis of Dimeric 22-kDa-ApoE3 by Nonreducing Gel Electrophoresis

To determine the ratio of dimeric 22-kDa-ApoE3 in the solution, Western blot analysis was performed under nonreducing conditions. Dimeric 22-kDa-ApoE3 was mixed with the same volume of a 2× nonreducing Laemmli buffer consisting of 100 mM Tris-HCl (pH 7.4), 10% glycerol, 4% SDS, and 0.01% bromophenol blue, and analyzed by 4–12% Tris/Tricine sodium dodecyl sulfate–polyacrylamide gel electrophoresis (SDS-PAGE) (Daiichi Pure Chemicals Co., Tokyo, Japan). The separated proteins were transferred onto Immobilon membranes with a semidry electrophoretic transfer apparatus (Nihon Eido, Tokyo, Japan) with a transfer buffer (0.1 M Tris-HCl (pH 7.4), 0.192 M glycine, and 20% methanol). The blots were probed for 16 hr at 4°C with a goat anti-ApoE polyclonal antibody, AB947 (1:2,000; Chemicon, Temecula, CA). Band detection was carried out with an ECL kit (GE Healthcare UK Ltd., England).

Purification and Carboxamidomethylation of Recombinant Intact ApoE3

ApoE3 was dissolved in 5 M guanidine–HCl, 10 mM EDTA, 200 mM Tris-HCl (pH8.5), and half of each protein solution was reduced with 10 mM DTT at room temperature for 2 hr and alkylated with 40 mM iodoacetamide in the dark at room temperature for 30 min, as described previously (Franceschini et al., 1990). All the proteins were then purified on an Aquapore RP300 column (2.1 × 30 mm; Applied Biosystems; Foster City, CA) by reverse-phase high-performance liquid chromatography (HPLC; model 1100 Series; Agilent Technology, Waldbronn, Germany) with a linear gradient of 36–52% acetonitrile in 0.1% trifluoroacetic acid for 16 min and a linear gradient of 52–76% acetonitrile in 0.1% trifluoroacetic acid for 1 min at a flow rate of 0.2 ml/min. The HPLC-purified ApoE3 was lyophilized and kept at −30°C until use.

Effect of 22-hydroxycholesterol and Glyburide on 22-kDa-ApoEs-induced Lipid Efflux

Neuron cultures were prepared, maintained, and labeled with [^{14}C]acetate, and exposed to 22-kDa-ApoE3 dimer or 22-kDa-ApoE3 monomer at a concentration of 0.3 μM in the presence of 22-hydroxycholesterol (10 μM) or glyburide (500 μM) for 24 hr. The lipids released into the media and the lipids retained in the cells were then determined. The expression level of ABCA1 in the cultures for each treatment was determined by Western blot analysis with anti-ABCA1 antibody (Santa Cruz, Santa Cruz, CA) used as a primary antibody.

RNA Interference

To knock down the endogenous ABCA1, primary cultured neurons and astrocytes were transiently transfected with 50 nM of the synthesized small interfering RNAs (siRNAs) targeting ABCA1 or with the Stealth siRNA negative control (Invitrogen) with Lipofectamine RNAiMAX (Invitrogen) according to the manufacturer's protocol. ABCA1 siRNA sequences is as follows: ABCA1-siRNA sense (5′-CAGGAUUUCCUGGUGGACAAUGAAA-3′) and antisense (5′-UUUCAUUGUCCACCAGGAAAUCCUG-3′).

Statistical Analysis

StatView computer software (Windows) was used for statistical analysis. The statistical significance of differences between samples was evaluated by multiple pairwise comparisons among the sets of data by ANOVA and the Bonferroni *t*-test.

RESULTS

Primary-cultured neurons and astrocytes were prepared and the levels of cholesterol and PC efflux were determined as described in Experimental Procedures. The levels of cholesterol and PC released from neurons in the medium treated with ApoE3 at 0.3 μM were significantly greater than those in the medium treated with ApoE4 (Fig. 1A). The level of cholesterol released by ApoE4 was 25% of that released by ApoE3. The reduced levels of cholesterol and PC efflux induced by ApoE4 increased significantly, although not to the level induced by ApoE3, when the neurons were incubated with the apoE4 (E255A) mutant (mt-ApoE4), which has altered amino- and carboxyl-terminal domain interaction because there is no electrostatic interaction between Arg61 and Glu255 (Dong and Weisgraber, 1996) (Fig. 1A). The partial recovery in the level of lipid efflux induced by mt-ApoE4 suggests that mechanisms other than the domain interaction are involved in ApoE-isoform-dependent lipid efflux from neurons in culture. Similar results were observed with cultured astrocytes. The levels of cholesterol and PC released from astrocytes in the medium treated with ApoE3 at 0.3 μM were significantly greater than those in the medium treated with ApoE4 (Fig. 1B). The levels of cholesterol and PC efflux induced by ApoE4 increased significantly, although not to the level induced by ApoE3, when the astrocytes were incubated with mt-ApoE4 (Fig. 1B).

We also examined the effect of the ApoE fragments on lipid efflux from cultured neurons and astrocytes to determine which part of the ApoE molecule is responsible for lipid efflux and ApoE isoform dependency. Interestingly, the 22-kDa fragment of ApoE (22-kDa-ApoE) induced cholesterol and PC efflux, which were ApoE-isoform-dependent (Fig. 1A,B). Unexpectedly, the carboxyl-terminal 10-kDa-ApoE and 12-kDa-ApoE, both of which contain the lipid binding site, have a very weak ability to release lipids (Fig. 1A,B).

Figure 2A shows the time-dependent cholesterol and PC efflux from neurons induced by 22-kDa-ApoE3 and 22-kDa-ApoE4 at 0.3 μM. The level of lipids released by 22-kDa-ApoE3 was significantly greater than that by 22-kDa-ApoE4 at time points of 24 and 48 hr (Fig. 2B). The level of cholesterol and PC efflux induced by 22-kDa-ApoE 24 hr after the treatment increased in an ApoE-concentration-dependent manner (Fig. 2B). The levels of cholesterol and PC efflux induced by 22-kDa-ApoE3 were greater than those released by 22-kDa-ApoE4 at 0.3 and 1.0 μM (Fig. 2B). Time- and ApoE-dose-dependent lipid efflux was also examined with ApoE-deficient astrocyte cultures, and the similar results were observed (Fig. 2C,D).

The results in Figures 1 and 2 indicate that the amino-terminal domain, the 22-kDa fragment, induces lipid efflux in an ApoE-isoform dependent manner, whereas the carboxyl-terminal domain, the 10-kDa fragment, has a very weak ability to induce lipid efflux from cultured astrocytes. These results raise the question of how the amino-terminal and carboxyl-terminal domains

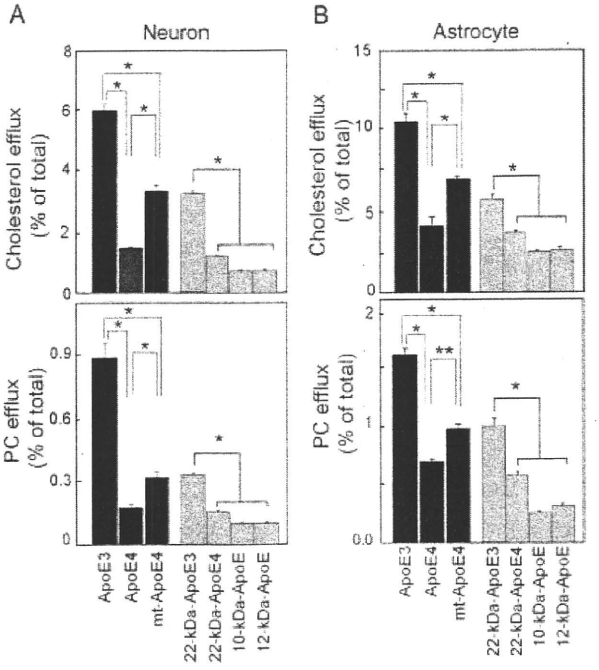

Fig. 1. Cholesterol and PC efflux from cultured neurons and astrocytes induced by ApoEs. Neurons and astrocytes were prepared as described in Experimental Procedures. The neurons (**A**) and astrocytes (**B**) were cultured for 72 hr, labeled with [^{14}C]acetate for 48 hr, and exposed to intact, lipid-free, ApoE3(residues 1–299), ApoE4, mt-ApoE4(E255A), 22-kDa-ApoE3 (residues 1–191), 22-kDa-ApoE4, 10-kDa-ApoE (residues 218–299), and 12-kDa-ApoE (residues 192–299) fragments at 0.3 μM for 24 hr. The lipids released into the media and the lipids retained in the cells were extracted and analyzed as described in Experimental Procedures. The percentages of released cholesterol and PC levels over the total levels were calculated. Data are means ± SE of four samples. $*P < 0.0001$ and $**P < 0.0005$. Three independent experiments showed similar results. The basal value of cholesterol and PC efflux in the absence of ApoEs are 1.0 ± 0.1 (%) and 0.4 ± 0.1 (%), respectively.

contribute to lipid efflux induced by intact ApoE in an ApoE-isoform-dependent manner. To answer this question, we examined whether the carboxyl-terminal domain of ApoE modifies lipid efflux caused by 22-kDa-ApoE. The ApoEs used were 22-kDa-ApoE (amino acids, 1–191) and 22-kDa-ApoE with carboxyl-terminal fragment of various lengths, that is, ApoEs harboring amino acids 1–250, 1–260, 1–272, and 1–299 (intact ApoE). As shown in Figure 3A, cholesterol and PC efflux induced by ApoE3 species from cultured neurons depended on the carboxyl-terminal fragment length; that is, ApoE3 variants with a longer carboxyl-terminal region induced progressively more lipid efflux. However, such is not the case for ApoE4. The addition of a carboxyl-terminal region ending at amino acid 250 increased the level of lipid efflux significantly more than 22-kDa-ApoE4; however, 22-kDa-ApoE4 with a car-

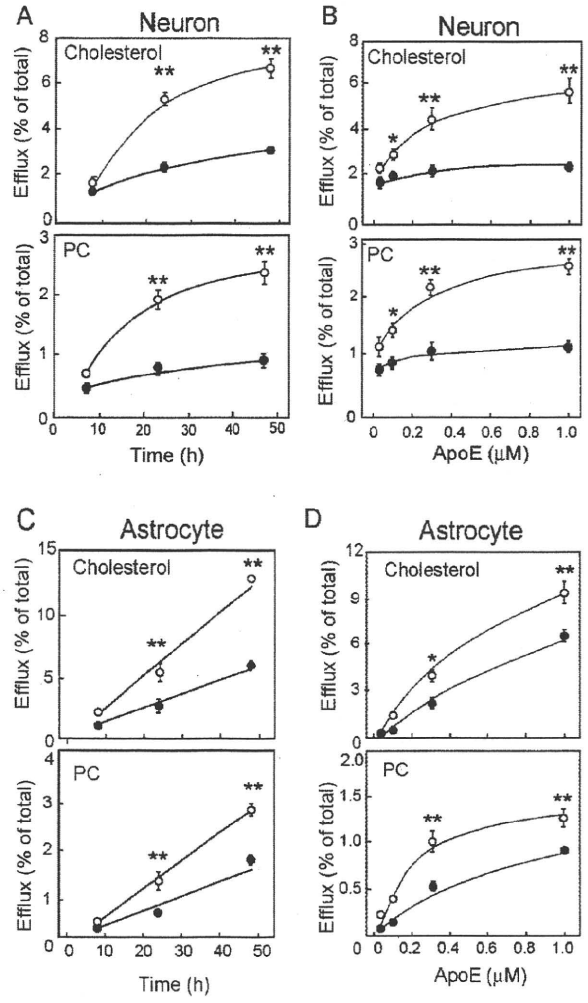

Fig. 2. Time- and dose-dependent lipid efflux mediated by 22-kDa-ApoE fragment. Cultured neurons and astrocytes were prepared, maintained, and labeled with [^{14}C]acetate as described in the legend for Fig. 1. For determination of the time-dependent lipid release from neurons (**A**) and astrocytes (**C**), each culture was exposed to 22-kDa-ApoE3 (open circle) and 22-kDa-ApoE4 (closed circle) at 0.3 μM for 8, 24, and 48 hr. For determination of the dose-dependent lipid release from neurons (**B**) and astrocytes (**D**), each culture was exposed to 22-kDa-ApoE3 (open circle) and 22-kDa-ApoE4 (closed circle) at varying concentrations for 24 hr. The lipids released into the media and the lipids retained in the cells were determined as described in Experimental Procedures. (**B**) For determination of Data are means ± SE of four samples. $*P < 0.05$ and $**P < 0.0005$ vs. 22-kDa-ApoE4 at each time point. The basal value of cholesterol and PC efflux in the absence of ApoEs are less than 0.8 ± 0.05 and 0.66 ± 0.11, respectively (**A**), and 0.59 ± 0.04 and 0.39 ± 0.04, respectively (**B**).

boxyl- terminal region longer than 250 amino acid residues lost the additional effect of the carboxyl-terminal region on lipid efflux. The levels of cholesterol and PC efflux induced by mt-ApoE4 recovered significantly but partially, and they did not reach those induced by intact ApoE3, similar to the result shown in Figure 1. Similar results were observed when ApoE-deficient astrocyte cultures were used (Fig. 3B).

The above results suggest that the amino-terminal domain basically determines the ability of ApoE to induce lipid efflux and that the carboxyl-terminal region enhances this ability when the amino and carboxyl domain interaction is absent. Because the absence or presence of cysteine at position 112 in the amino-terminal domain differentiates ApoE3 from ApoE4, it is possible to assume that this one-amino-acid difference results in intra- or intermolecular structural differences leading to the domain interaction or dimerization, respectively. Thus, we examined the effect of the dimer formation of 22-kDa-ApoE3 through disulfide bonds on lipid efflux from neurons and cultured astrocytes. To determine directly whether the dimeric form of 22-kDa-ApoE3 induces greater lipid efflux from astrocytes than the monomeric form, the pure dimeric form of 22-kDa-ApoE3 was prepared as described in Experimental Procedures. To obtain a solution containing the pure monomeric form of 22-kDa-ApoE3, 22-kDa-ApoE3 was dissolved in 5 M guanidine–HCl and 10 mM DTT. The resulting solutions were dialyzed against PBS at 4°C for 16 hr and used for the experiment. The purity of dimer and monomer in each sample was confirmed by Western blot analysis (Fig. 4). We also used 22-kDa-ApoE4 as monomeric ApoE molecule for the experiment that used astrocyte cultures because 22-kDa-ApoE4 contains no cysteine and it remains monomeric (Fig. 4B). The results demonstrated that dimeric form of 22-kDa-ApoE3 induced greater lipid efflux than the monomeric form of 22-kDa-ApoE3 and 22-kDa-ApoE4 in both neuron and astrocyte cultures (Fig. 4). Importantly, regardless of ApoE isoform, monomeric 22-kDa-ApoEs induces similar level of lipid efflux (Fig. 4B).

To determine whether such is the case for intact ApoEs, we examined the effect of the dimer formation of ApoE3 through disulfide bonds on lipid efflux from cultured neurons. We obtained dimer-enriched ApoE3 solutions by using a SulfoLink kit as described under Experimental Procedures. We also used ApoE3 solutions prepared without dimer enrichment, containing monomers and relatively few dimers. We also examined the effect of monomeric ApoEs, namely ApoE4 and ApoE3, whose cysteine was modified by carboxamidomethylation (ApoE3-CM). The levels of cholesterol and PC released from neurons treated with dimer-enriched ApoE3 were 2.9- and 7.6-fold greater than those released from neurons treated with ApoE3 and ApoE3 monomers (ApoE3-CM), respectively (Fig. 5). The effects of ApoE3-CM and ApoE4 on lipid efflux were similar. A Western blot analysis of each sample was performed and results show that the samples contained different amounts of dimers (Fig. 5B). The percentages of ApoE3 dimers as calculated by a densitometric analysis of the bands on the Western blot films were 64.5%,

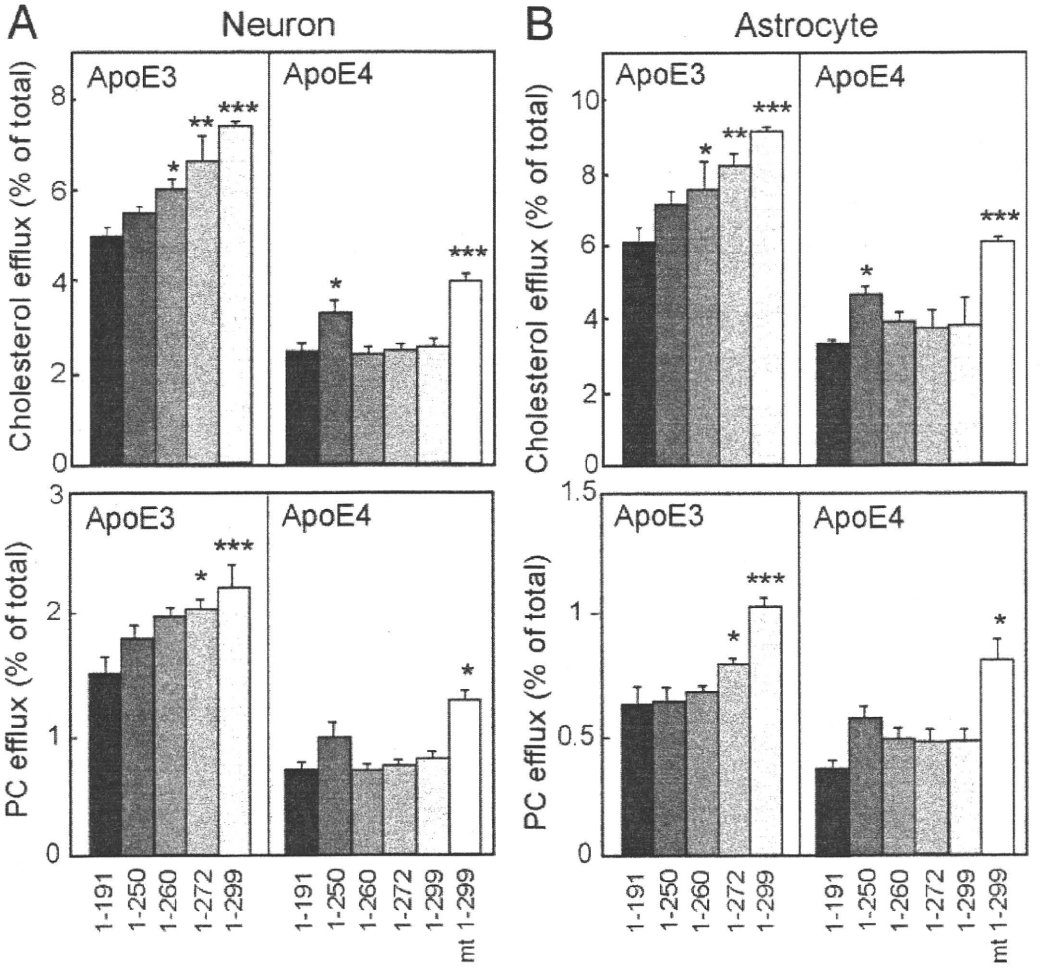

Fig. 3. Cooperative effects of amino- and carboxyl-terminal regions of ApoE on lipid efflux. Neurons and astrocytes were prepared, maintained, and labeled with [^{14}C]acetate as described in the legend for Fig. 1. The neurons (**A**) and astrocytes (**B**) were then exposed to ApoE with carboxyl-terminal regions of various lengths including 1–250, 1–260, 1–272, and 1–299 (full-length ApoE) at 0.3 μM for 24 hr, and the lipids released into the media and the lipids retained in the cells were determined as described in Experimental Procedures. For comparison, the effect of mt-ApoE4 was also determined. Data are means ± SE of four samples. $*P < 0.05$, $**P < 0.005$, and $***P < 0.0001$ vs. 22-kDa-ApoE (1–191). The basal value of cholesterol and PC efflux in the absence of ApoEs are less than 0.8 ± 0.05 and 0.66 ± 0.11, respectively (A, B).

36.9%, 1.8%, and 1.4% in the dimer-enriched ApoE3, non-dimer-enriched ApoE3, ApoE3-CM, and ApoE4 samples, respectively.

Next we determined the involvement of ABCA1 in 22-kDa-ApoEs-induced lipid efflux. The neuron cultures were treated with 22-kDa-ApoE3 dimers, 22-kDa-ApoE3 monomers, or 22-kDa-ApoE4 (monomers) concomitant with 10 μM of 22-hydroxycholesterol, an LXR ligand to up-regulate *ABCA1* gene expression (Wang et al., 2001), and the cultures were maintained for 24 hr. After 24 hr incubation, the level of lipids released into the medium was determined. The ABCA1 expression level was enhanced when the neurons were treated with 22-hydroxycholesterol (Fig. 6A). The levels of lipids released by these ApoE fragments were significantly enhanced when the cultures were concomitantly treated with 22-hydroxycholesterol (Fig. 6B). These results suggest that ABCA1 plays a key role in 22-kDa-ApoEs-mediated lipid efflux in neurons. In support of this notion, we have observed that the treatment of neurons with glyburide, an inhibitor of the ABCA1 transporter, resulted in decreased levels of 22-kDa-ApoE3-mediated cholesterol efflux (Fig. 6C). We further examined the effect of ABCA1 knockdown on 22-kDa ApoEs-mediated lipid efflux by using specific siRNAs. The knockdown of ABCA1 in neurons significantly reduced lipid efflux induced by 22-kDa-ApoE3 dimers (Fig. 7).

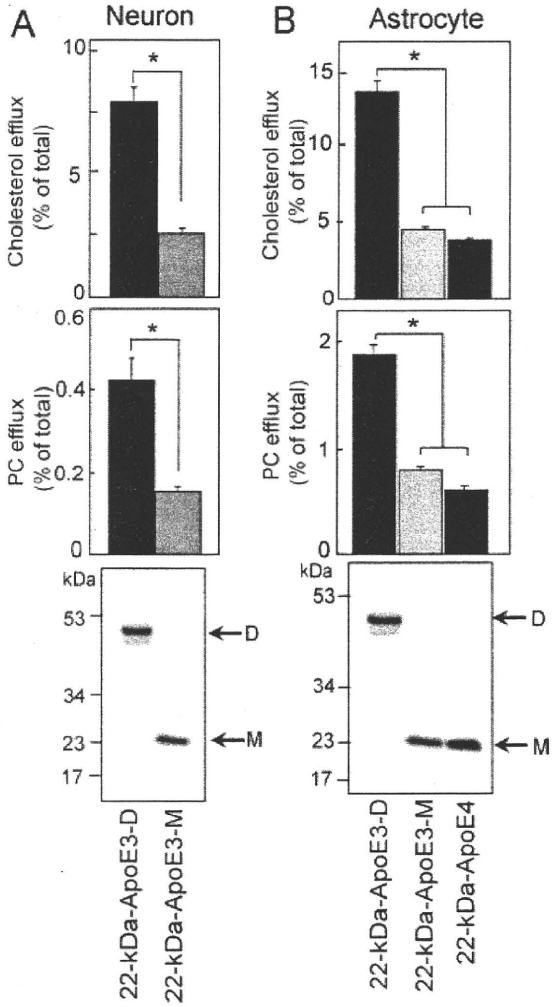

Fig. 4. The ability of 22-kDa-ApoE to induce lipid efflux depends on the ApoE self-association state, i. e., monomer vs dimer. Preparation of 22-kDa-ApoE3 dimer (22-kDa-ApoE3-D), monomer (22-kDa-ApoE3-M), or 22-kDa-ApoE4 monomer was performed as described in Experimental Procedures. **A:** The same amount of 22-kDa-ApoE3-D or 22-kDa-ApoE3-M was subjected to SDS-PAGE under nonreducing conditions, and Western blot analysis was performed with the anti-ApoE antibody AB947. D; dimers, M; monomer. Neuron cultures were prepared, maintained, and labeled with [^{14}C]acetate and exposed to 22-kDa-ApoE3-D or 22-kDa-ApoE3-M at 0.3 μM for 24 hr. The cholesterol and PC efflux by dimeric and monomeric 22-kDa-ApoE3 was determined. **B:** The same amount of 22-kDa-ApoE3 dimers, 22-kDa-ApoE3 monomers, and 22-kDa-ApoE4 monomers was subjected to SDS-PAGE under nonreducing conditions, and Western blot analysis was performed with the anti-ApoE antibody AB947. D; dimers, M; monomer. Astrocyte cultures were prepared, maintained, and labeled with [^{14}C]acetate and exposed to 22-kDa-ApoE3-D, 22-kDa-ApoE3-M, or 22-kDa-ApoE4 monomer at 0.3 μM for 24 hr. The cholesterol and PC efflux by dimeric and monomeric 22-kDa-ApoE3, and monomeric 22-kDa-ApoE4 was determined. Data are means ± SE of four samples. $*P < 0.0001$ vs. 22-kDa-ApoE3. The basal value of cholesterol and PC efflux in the absence of ApoEs are less than 1.41 ± 0.06 and 0.55 ± 0.03, respectively (A, B).

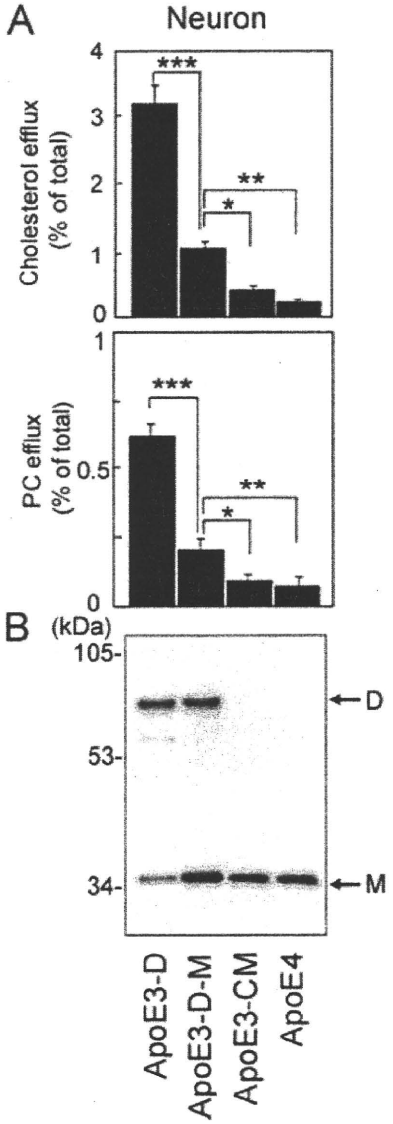

Fig. 5. Effect of intact ApoE dimers on lipid efflux from cultured neurons. A dimer-rich ApoE3 solution was obtained with a column that traps SH residues (monomeric ApoE3s). Carboxamidomethylated ApoE with iodoacetamide was prepared as described in Experimental Procedures. Neuronal cultures were prepared, maintained, and labeled with [^{14}C]acetate and exposed to dimer-enriched ApoE3, ApoE3, ApoE3-CM, and ApoE4 at 0.3 μM for 24 hr. **A:** The levels of cholesterol and PC released into the media and those retained in the cells were determined as described in Experimental Procedures. **B:** To determine the amount of dimers in the samples, Western blot analysis was performed under nonreducing conditions with anti-ApoE antibody AB947 used as the primary antibody. Data are means ± SE of four samples. $*P < 0.01$, $**P < 0.001$, $***P < 0.0001$. The basal value of cholesterol and PC efflux in the absence of ApoEs are 1.54 ± 0.05 and 0.56 ± 0.05, respectively.

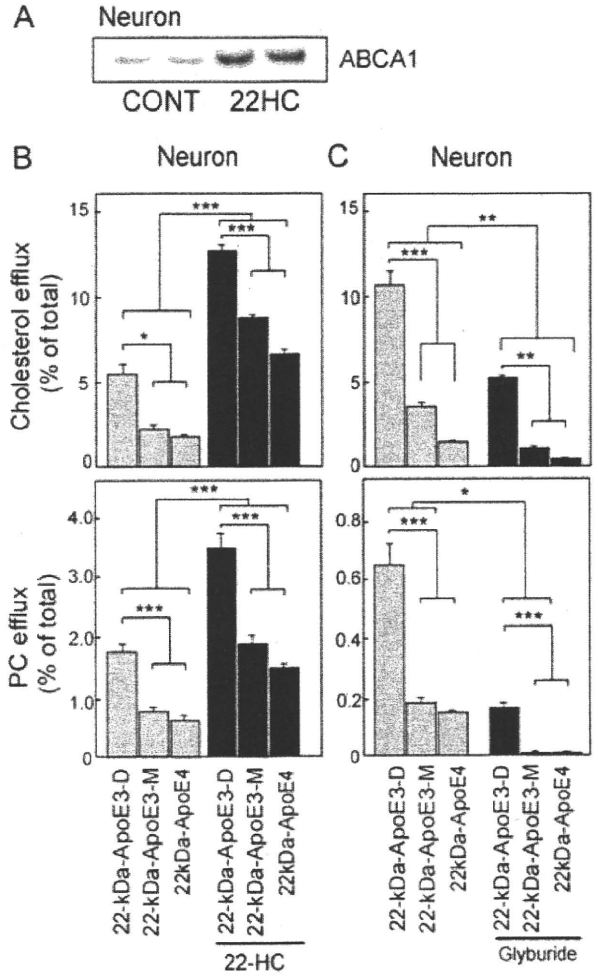

Fig. 6. The effect of 22-hydroxycholesterol and glyburide on 22-kDa-ApoEs-induced lipid efflux. Neuron cultures were prepared, maintained, and labeled with [^{14}C]acetate as described in Fig. 1, and exposed to 22-kDa-ApoE3 dimer (22-kDa-ApoE3-D), 22-kDa-ApoE3 monomer (22-kDa-ApoE3-M), or 22-kDa-ApoE4 at a concentration of 0.3 μM in the presence of 22-hydroxycholesterol (HC) at a concentration of 10 μM for 24 hr. (**A**) The expression level of ABCA1 in the cultures for each treatment was determined by Western blot analysis, and (**B**) the lipids released into the media and the lipids retained in the cells were determined. (**C**) [^{14}C]acetate-labeled neuron cultures were exposed to 22-kDa-ApoE3 dimer (22-kDa-ApoE3-D), 22-kDa-ApoE3 monomer (22-kDa-ApoE3-M), or 22-kDa-ApoE4 at a concentration of 0.3 μM in the presence of glyburide (500 μM) for 24 hr. The lipids released into the media and the lipids retained in the cells were determined. Data are means ± SE of four samples. $*P < 0.05$, $**P < 0.01$, and $***P < 0.0005$. Three independent experiments showed similar results. The basal value of cholesterol and PC efflux in the absence of ApoEs are 5.45 ± 0.51 and 0.58 ± 0.06, respectively.

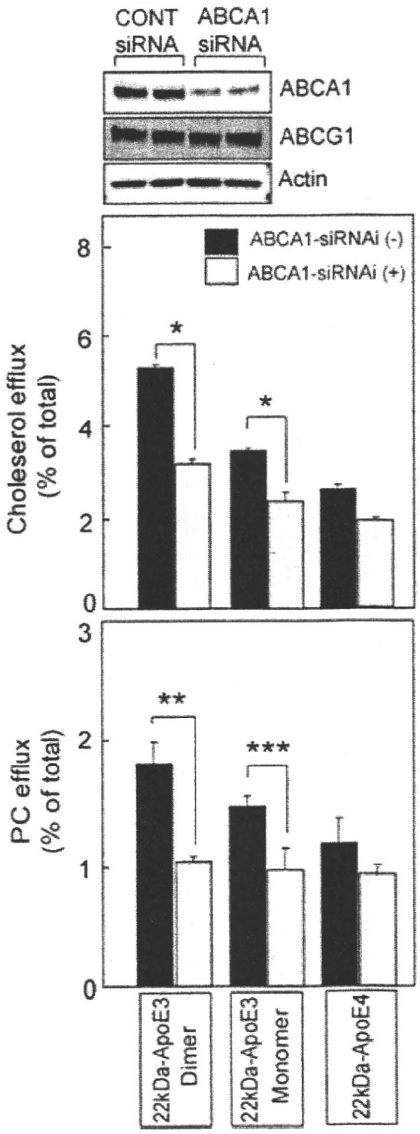

Fig. 7. Lipid efflux by 22-kDa-ApoEs is mediated by ABCA1. The primary neurons, which had been labeled with [^{14}C]acetate and treated with siRNA against ABCA1 for 48 hr, were exposed to 22-kDa-ApoE3 dimer (22-kDa-ApoE3-D) or 22-kDa-ApoE3 monomer (22-kDa-ApoE3-M) at a concentration of 0.3 μM, and maintained for 24 hr. The lipids released into the media and the lipids retained in the cells were then determined as described in Experimental Procedures. Data are means ± SE of four samples. $*P < 0.0001$, $**P < 0.002$, $***P < 0.02$. Three independent experiments showed similar results. The basal value of cholesterol and PC efflux in the absence of ApoEs are 0.89 ± 0.08 and 0.97 ± 0.14, respectively. Those values are 0.84 ± 0.08 and 0.46 ± 0.07 in the siABCA1 experiment.

DISCUSSION

We showed here that lipid efflux induced by ApoE is mainly mediated by the amino-terminal domain of ApoE and modified by the carboxyl-terminal domain. What we found are that the amino-terminal domain of ApoE induces lipid efflux in an isoform-dependent manner and the carboxyl-terminal domain enhances lipid efflux mediated by the amino-terminal domain of ApoE3. In contrast, the carboxyl-terminal domain does not strengthen the lipid efflux mediated by the amino-terminal domain of ApoE4 because of the domain interaction between the amino- and carboxyl-terminal domains. We also found that the lipid efflux induced by these ApoEs is mediated in an ABCA1-dependent manner.

Two of the main findings in this study are that the amino-terminal domain of ApoE, 22-kDa-ApoE, induces lipid efflux and that the extent of lipids released by the amino-terminal domain of ApoE, 22-kDa-ApoE3, is approximately 66% of that induced by intact ApoE3. The carboxyl-terminal domain synergistically and additively modifies lipid efflux mediated by 22-kDa-ApoE3. The additional contribution of the carboxyl-terminal domain is not observed in the case of ApoE4. Basically, 22-kDa-ApoE4 has a very weak ability to induce lipid efflux; moreover, the carboxyl-terminal region of ApoE does not effectively or additively enhance the lipid efflux mediated by 22-kDa-ApoE4. The lack of an additive effect by the carboxyl-terminal region on lipid efflux is likely due to the domain interaction, because an ApoE4 fragment ending at 250 (ApoE1–250) significantly gains in ability to release lipids; however, a carboxyl-terminal region longer than the amino acid 255, glutamate, which interacts with arginine at 61 (called the domain interaction; Dong and Weisgraber, 1996), does not induce any additive effect on lipid efflux induced by 22-kDa-ApoE4.

Another important finding regarding the effect of the domain interaction is that lipid efflux induced by mt-ApoE4 shows only a partial recovery toward the level exhibited by ApoE3. This indicates that the presence or absence of the amino and carboxyl domain interaction cannot completely explain ApoE-isoform-dependent lipid efflux mediated by intact ApoE and that other mechanisms are responsible for such ApoE-isoform dependency. This is supported by the finding of this study that 22-kDa-ApoE, which has no carboxyl-terminal region and thus has no domain interaction, induces lipid release in an ApoE-isoform-dependent manner.

We have already shown that α-helix formation is required for the high-affinity binding of apolipoprotein A-I to lipids (Saito et al., 2004), and that the binding capacity of 22-kDa-ApoE3 is lower than that of 22-kDa-ApoE4 for lipid particles (Saito et al., 2003). On the basis of the facts that the structural stabilities of 22-kDa-ApoE3 and 22-kDa-ApoE4 determine their binding affinity to lipids (Morrow et al., 2002; Segall et al., 2002; Weers et al., 2003) and that 22-kDa-ApoE4 is less stable than 22-kDa-ApoE3 (Morrow et al., 2000), it is reasonable to predict that the level of lipid efflux induced by 22-kDa-ApoE4 would be greater than that induced by 22-kDa-ApoE3. However, our results show the opposite, indicating that ApoE-isoform-dependent cholesterol efflux is unlikely to be explained by a simple theory linking the structural difference between these two fragments with their binding affinity to lipids.

Therefore, the question arises as to what is the mechanism underlying the isoform dependency of 22-kDa-ApoE-induced lipid efflux. It is possible to assume that 22-kDa-ApoE induces lipid efflux, because the 22-kDa domain contains an amphipathic four-helix bundle (Wilson et al., 1991), and it can bind to and reorganize phospholipid vesicles to form discoidal complexes (Lu et al., 2000; Segall et al., 2002). Surprisingly, 22-kDa-ApoE-induced lipid efflux is ApoE-isoform dependent. Such isoform dependency is likely to be caused by the presence or absence of cysteine at residue 112, which may result in intra- or intermolecular structural changes, forming dimers of 22-kDa-ApoE through disulfide bonds. More direct evidence that the dimeric form of 22-kDa-ApoE3 induces greater lipid efflux from cultured neurons and astrocytes than the monomeric form (Fig. 4) supports this idea. Previous reports have demonstrated that cellular cholesterol efflux is induced by many apolipoproteins in their lipid-free form, including ApoA-I, ApoA-II, ApoA-IV, and ApoCIII in addition to ApoE, all of which harbor multiple segments of amphiphilic helices (Segrest et al., 1992); the reaction still occurs with shorter apolipoproteins but to a lesser extent and only at high concentrations (Bielicki et al., 1992). Synthetic amphipathic helical peptides that mimic the physical properties of amphipathic helical segments of apolipoproteins can also induce cholesterol efflux as long as the peptide has at least two such helical segments (Mendez et al., 1994; Yancey et al., 1995). Consistent with these lines of evidence, when human ApoA-II, a disulfide-linked dimer, is reduced to a carboxyamidomethylation monomeric form, the ability of ApoA-II to induce cholesterol efflux is significantly decreased (Hara et al., 1992). In addition, the disulfide- linked homodimer of ApoE3 has been identified not only in cell culture medium (Gong et al., 2002), but also in human plasma (Weisgraber and Shinto, 1991). The mechanism by which the ApoE and ApoA-II dimers gain their functions to release higher amounts of lipids than ApoE and ApoA-II monomers, respectively, remains to be elucidated.

ABCA1 is involved in apolipoprotein-induced lipid efflux, including that mediated by ApoA-I (Brooks-Wilson et al., 1999; Lawn et al., 1999) and ApoE (Remaley et al., 2001; Krimbou et al., 2004). Regarding its effect on lipid efflux, the carboxyl-terminal fragment of ApoE (10-kDa-ApoE) induces a strong lipid efflux from non-CNS cells such as macrophages and ABCA1 plays a critical role in this efflux (Vedhachalam et al., 2007). Interestingly, contrary to these findings, 10-kDa-ApoE does not induce lipid efflux from the cultured neurons and astrocytes (Fig. 1). The reason for this discrepancy

remains unknown; however, the cell type difference may be a likely reason. In support of this notion, even intact ApoE3 induces a very low level of lipid efflux from macrophages or fibroblasts, and ABCA1 transfection induces a marked lipid efflux mediated by intact ApoE3 in these cells (Smith et al., 1996; Remaley et al., 2001). In contrast, intact ApoE3 itself induces marked lipid efflux from astrocytes without ABCA1 transfection as shown in this study. This may be because apolipoprotein-mediated cholesterol efflux is only apparent in growth-arrested cells (Mendez, 1997).

We have observed that pretreatment with 22-hydroxylcholesterol enhanced ABCA1 expression in neurons and cholesterol efflux induced by ApoE, suggesting that ABCA1 is involved in ApoE- and 22-kDa-ApoE3-mediated cholesterol efflux (Fig. 6). The involvement of ABCA1 has been also demonstrated by the fact that the knockdown of ABCA1 significantly reduced lipid efflux induced by 22-kDa ApoEs (Fig. 7). One cannot exclude the possibility that factors other than ABCA1 that are relevant to biological mechanisms are involved because the involvement of ATP-binding cassette protein G1 has been reported previously (Karten et al., 2006; Kim et al., 2007); however, the lines of evidence in our present study suggest that lipid efflux from cultured neurons induced by ApoE or an ApoE fragment is mediated by ABCA1 function.

It is reasonable to assume that the disruption of the ApoE4 domain interaction by, for example, small molecules that create the ApoE3-like structure is a potential therapeutic target in neurodegenerative diseases including AD (Mahley et al., 2006). However, if the role of ApoE in HDL generation and its supply to neurons are critically involved in neurodegeneration in AD, other approaches that do not modulate the acceptor function, but modulate the cellular factors including ABCA1 expression and subsequent HDL generation, could also be candidate therapeutic targets.

REFERENCES

Bielicki JK, Johnson WJ, Weinberg RB, Glick JM, Rothblat GH. 1992. Efflux of lipid from fibroblasts to apolipoproteins: dependence on elevated levels of cellular unesterified cholesterol. J Lipid Res 33:1699–1709.

Borghini I, Barja F, Pometta D, James RW. 1995. Characterization of subpopulations of lipoprotein particles isolated from human cerebrospinal fluid. Biochim Biophys Acta 1255:192–200.

Boyles JK, Pitas RE, Wilson E, Mahley RW, Taylor JM. 1985. Apolipoprotein E associated with astrocytic glia of the central nervous system and with nonmyelinating glia of the peripheral nervous system. J Clin Invest 76:1501–1513.

Brooks-Wilson A, Marcil M, Clee SM, Zhang LH, Roomp K, van Dam M, Yu L, Brewer C, Collins JA, Molhuizen HO, Loubser O, Ouelette BF, Fichter K, Ashbourne-Excoffon KJ, Sensen CW, Scherer S, Mott S, Denis M, Martindale D, Frohlich J, Morgan K, Koop B, Pimstone S, Kastelein JJ, Hayden MR. 1999. Mutations in ABC1 in Tangier disease and familial high-density lipoprotein deficiency. Nat Genet 22: 336–345.

Corder EH, Saunders AM, Strittmatter WJ, Schmechel DE, Gaskell PC, Small GW, Roses AD, Haines JL, Pericak-Vance MA. 1993. Gene dose of apolipoprotein E type 4 allele and the risk of Alzheimer's disease in late onset families [see comments]. Science 261:921–923.

Demeester N, Castro G, Desrumaux C, De Geitere C, Fruchart JC, Santens P, Mulleners E, Engelborghs S, De Deyn PP, Vandekerckhove J, Rosseneu M, Labeur C. 2000. Characterization and functional studies of lipoproteins, lipid transfer proteins, and lecithin:cholesterol acyltransferase in CSF of normal individuals and patients with Alzheimer's disease. J Lipid Res 41:963–974.

Dong LM, Weisgraber KH. 1996. Human apolipoprotein E4 domain interaction. Arginine 61 and glutamic acid 255 interact to direct the preference for very low density lipoproteins. J Biol Chem 271:19053–19057.

Franceschini G, Calabresi L, Tosi C, Gianfranceschi G, Sirtori CR, Nichols AV. 1990. Apolipoprotein AIMilano. Disulfide-linked dimers increase high density lipoprotein stability and hinder particle interconversion in carrier plasma. J Biol Chem 265:12224–12231.

Gong JS, Kobayashi M, Hayashi H, Zou K, Sawamura N, Fujita SC, Yanagisawa K, Michikawa M. 2002. Apolipoprotein E (ApoE) isoform-dependent lipid release from astrocytes prepared from human ApoE3 and ApoE4 knock-in mice. J Biol Chem 277:29919–29926.

Hara H, Komaba A, Yokoyama S. 1992. Alpha-helical requirements for free apolipoproteins to generate HDL and to induce cellular lipid efflux. Lipids 27:302–304.

Hatters DM, Budamagunta MS, Voss JC, Weisgraber KH. 2005. Modulation of apolipoprotein E structure by domain interaction: differences in lipid-bound and lipid-free forms. J Biol Chem 280:34288–34295.

Karten B, Campenot RB, Vance DE, Vance JE. 2006. Expression of ABCG1, but not ABCA1, correlates with cholesterol release by cerebellar astroglia. J Biol Chem 281:4049–4057.

Kim WS, Rahmanto AS, Kamili A, Rye KA, Guillemin GJ, Gelissen IC, Jessup W, Hill AF, Garner B. 2007. Role of ABCG1 and ABCA1 in regulation of neuronal cholesterol efflux to apolipoprotein E discs and suppression of amyloid-beta peptide generation. J Biol Chem 282:2851–2861.

Krimbou L, Denis M, Haidar B, Carrier M, Marcil M, Genest J Jr. 2004. Molecular interactions between apolipoprotein E and the ATP-binding cassette transporter A1 (ABCA1): impact on ApoE lipidation. J Lipid Res 46:1457–1465.

LaDu MJ, Gilligan SM, Lukens JR, Cabana VG, Reardon CA, Van Eldik LJ, Holtzman DM. 1998. Nascent astrocyte particles differ from lipoproteins in CSF. J Neurochem 70:2070–2081.

Lawn RM, Wade DP, Garvin MR, Wang X, Schwartz K, Porter JG, Seilhamer JJ, Vaughan AM, Oram JF. 1999. The Tangier disease gene product ABC1 controls the cellular apolipoprotein-mediated lipid removal pathway. J Clin Invest 104:R25–31.

Lu B, Morrow JA, Weisgraber KH. 2000. Conformational reorganization of the four-helix bundle of human apolipoprotein E in binding to phospholipid. J Biol Chem 275:20775–20781.

Mahley RW, Weisgraber KH, Huang Y. 2006. Apolipoprotein E4: a causative factor and therapeutic target in neuropathology, including Alzheimer's disease. Proc Natl Acad Sci U S A 103:5644–5651.

Mendez AJ. 1997. Cholesterol efflux mediated by apolipoproteins is an active cellular process distinct from efflux mediated by passive diffusion. J Lipid Res 38:1807–1821.

Mendez AJ, Anantharamaiah GM, Segrest JP, Oram JF. 1994. Synthetic amphipathic helical peptides that mimic apolipoprotein A-I in clearing cellular cholesterol. J Clin Invest 94:1698–1705.

Michikawa M, Fan QW, Isobe I, Yanagisawa K. 2000. Apolipoprotein E exhibits isoform-specific promotion of lipid efflux from astrocytes and neurons in culture. J Neurochem 74:1008–1016.

Michikawa M, Gong JS, Fan QW, Sawamura N, Yanagisawa K. 2001. A novel action of Alzheimer's amyloid b-protein (Ab): oligomeric Ab promotes lipid release. J Neurosci 21:7226–7235.

Molander-Melin M, Blennow K, Bogdanovic N, Dellheden B, Mansson JE, Fredman P. 2005. Structural membrane alterations in Alzheimer brains found to be associated with regional disease development: increased density of gangliosides GM1 and GM2 and loss of cholesterol in detergent-resistant membrane domains. J Neurochem 92:171–182.

Morrow JA, Segall ML, Lund-Katz S, Phillips MC, Knapp M, Rupp B, Weisgraber KH. 2000. Differences in stability among the human apolipoprotein E isoforms determined by the amino-terminal domain. Biochemistry 39:11657–11666.

Morrow JA, Hatters DM, Lu B, Hochtl P, Oberg KA, Rupp B, Weisgraber KH. 2002. Apolipoprotein E4 forms a molten globule. A potential basis for its association with disease. J Biol Chem 277:50380–50385.

Nakai M, Kawamata T, Taniguchi T, Maeda K, Tanaka C. 1996. Expression of apolipoprotein E mRNA in rat microglia. Neurosci Lett 211:41–44.

Pitas RE, Boyles JK, Lee SH, Foss D, Mahley RW. 1987a. Astrocytes synthesize apolipoprotein E and metabolize apolipoprotein E–containing lipoproteins. Biochim Biophys Acta 917:148–161.

Pitas RE, Boyles JK, Lee SH, Hui D, Weisgraber KH. 1987b. Lipoproteins and their receptors in the central nervous system. Characterization of the lipoproteins in cerebrospinal fluid and identification of apolipoprotein B,E(LDL) receptors in the brain. J Biol Chem 262:14352–14360.

Raffai RL, Dong LM, Farese RV Jr, Weisgraber KH. 2001. Introduction of human apolipoprotein E4 "domain interaction" into mouse apolipoprotein E. Proc Natl Acad Sci U S A 98:11587–11591.

Ramaswamy G, Xu Q, Huang Y, Weisgraber KH. 2005. Effect of domain interaction on apolipoprotein E levels in mouse brain. J Neurosci 25:10658–10663.

Remaley AT, Stonik JA, Demosky SJ, Neufeld EB, Bocharov AV, Vishnyakova TG, Eggerman TL, Patterson AP, Duverger NJ, Santamarina-Fojo S, Brewer HB Jr. 2001. Apolipoprotein specificity for lipid efflux by the human ABCAI transporter. Biochem Biophys Res Commun 280:818–823.

Roheim PS, Carey M, Forte T, Vega GL. 1979. Apolipoproteins in human cerebrospinal fluid. Proc Natl Acad Sci U S A 76:4646–4649.

Saito H, Dhanasekaran P, Baldwin F, Weisgraber KH, Lund-Katz S, Phillips MC. 2001. Lipid binding-induced conformational change in human apolipoprotein E. Evidence for two lipid-bound states on spherical particles. J Biol Chem 276:40949–40954.

Saito H, Dhanasekaran P, Baldwin F, Weisgraber KH, Phillips MC, Lund-Katz S. 2003. Effects of polymorphism on the lipid interaction of human apolipoprotein E. J Biol Chem 278:40723–40729.

Saito H, Dhanasekaran P, Nguyen D, Deridder E, Holvoet P, Lund-Katz S, Phillips MC. 2004. Alpha-helix formation is required for high affinity binding of human apolipoprotein A-I to lipids. J Biol Chem 279:20974–20981.

Segall ML, Dhanasekaran P, Baldwin F, Anantharamaiah GM, Weisgraber KH, Phillips MC, Lund-Katz S. 2002. Influence of apoE domain structure and polymorphism on the kinetics of phospholipid vesicle solubilization. J Lipid Res 43:1688–1700.

Segrest JP, Jones MK, De Loof H, Brouillette CG, Venkatachalapathi YV, Anantharamaiah GM. 1992. The amphipathic helix in the exchangeable apolipoproteins: a review of secondary structure and function. J Lipid Res 33:141–166.

Smith JD, Miyata M, Ginsberg M, Grigaux C, Shmookler E, Plump AS. 1996. Cyclic AMP induces apolipoprotein E binding activity and promotes cholesterol efflux from a macrophage cell line to apolipoprotein acceptors. J Biol Chem 271:30647–30655.

Strittmatter WJ, Saunders AM, Schmechel D, Pericak-Vance M, Enghild J, Salvesen GS, Roses AD. 1993. Apolipoprotein E: high-avidity binding to beta-amyloid and increased frequency of type 4 allele in late-onset familial Alzheimer disease. Proc Natl Acad Sci U S A 90:1977–1981.

Vedhachalam C, Narayanaswami V, Neto N, Forte TM, Phillips MC, Lund-Katz S, Bielicki JK. 2007. The C-terminal lipid-binding domain of apolipoprotein E is a highly efficient mediator of ABCA1-dependent cholesterol efflux that promotes the assembly of high-density lipoproteins. Biochemistry 46:2583–2593.

Wang N, Silver DL, Thiele C, Tall AR. 2001. ATP-binding cassette transporter A1 (ABCA1) functions as a cholesterol efflux regulatory protein. J Biol Chem 276:23742–23747.

Weers PM, Narayanaswami V, Choy N, Luty R, Hicks L, Kay CM, Ryan RO. 2003. Lipid binding ability of human apolipoprotein E N-terminal domain isoforms: correlation with protein stability? Biophys Chem 100:481–492.

Weisgraber KH. 1990. Apolipoprotein E distribution among human plasma lipoproteins: role of the cysteine–arginine interchange at residue 112. J Lipid Res 31:1503–1511.

Weisgraber KH, Shinto LH. 1991. Identification of the disulfide-linked homodimer of apolipoprotein E3 in plasma. Impact on receptor binding activity. J Biol Chem 266:12029–12034.

Weisgraber KH, Roses AD, Strittmatter WJ. 1994. The role of apolipoprotein E in the nervous system. Curr Opin Lipidol 5:110–116.

Wetterau JR, Aggerbeck LP, Rall SC Jr, Weisgraber KH. 1988. Human apolipoprotein E3 in aqueous solution. I. Evidence for two structural domains. J Biol Chem 263:6240–6248.

Wilson C, Wardell MR, Weisgraber KH, Mahley RW, Agard DA. 1991. Three-dimensional structure of the LDL receptor-binding domain of human apolipoprotein E. Science 252:1817–1822.

Xu Q, Brecht WJ, Weisgraber KH, Mahley RW, Huang Y. 2004. Apolipoprotein E4 domain interaction occurs in living neuronal cells as determined by fluorescence resonance energy transfer. J Biol Chem 279:25511–15516.

Yancey PG, Bielicki JK, Johnson WJ, Lund-Katz S, Palgunachari MN, Anantharamaiah GM, Segrest JP, Phillips MC, Rothblat GH. 1995. Efflux of cellular cholesterol and phospholipid to lipid-free apolipoproteins and class A amphipathic peptides. Biochemistry 34:7955–7965.

Molecular Neurodegeneration

BioMed Central

Research article

Open Access

Apolipoprotein E4 (1–272) fragment is associated with mitochondrial proteins and affects mitochondrial function in neuronal cells

Toshiyuki Nakamura[1], Atsushi Watanabe[2], Takahiro Fujino[3], Takashi Hosono[1] and Makoto Michikawa*[1]

Address: [1]Department of Alzheimer's Disease Research, National Institute for Longevity Sciences, National Center for Geriatrics and Gerontology, 36-3 Gengo, Morioka, Obu, Aichi 474-8522, Japan, [2]Department of Vascular Dementia, National Institute for Longevity Sciences, National Center for Geriatrics and Gerontology, 36-3 Gengo, Morioka, Obu, Aichi 474-8522, Japan and [3]Department of Bioscience, Integrated Center for Science (INCS), Ehime University, Shizukawa, Shigenobu-cyo, Onsengun, Ehime 791-0295, Japan

Email: Toshiyuki Nakamura - nakamu-t@nifty.com; Atsushi Watanabe - watsushi@nils.go.jp; Takahiro Fujino - tfujino@m.ehime-u.ac.jp; Takashi Hosono - t-hos@nils.go.jp; Makoto Michikawa* - michi@nils.go.jp

* Corresponding author

Published: 20 August 2009

Molecular Neurodegeneration 2009, **4**:35 doi:10.1186/1750-1326-4-35

Received: 8 July 2009
Accepted: 20 August 2009

This article is available from: http://www.molecularneurodegeneration.com/content/4/1/35

Abstract

Background: Apolipoprotein E allele ε4 (apoE4) is a strong risk factor for developing Alzheimer's disease (AD). Secreted apoE has a critical function in redistributing lipids among central nervous system cells to maintain normal lipid homeostasis. In addition, previous reports have shown that apoE4 is cleaved by a protease in neurons to generate apoE4(1–272) fragment, which is associated with neurofibrillary tanglelike structures and mitochondria, causing mitochondrial dysfunction. However, it still remains unclear how the apoE fragment associates with mitochondria and induces mitochondrial dysfunction.

Results: To clarify the molecular mechanism, we carried out experiments to identify intracellular apoE-binding molecules and their functions in modulating mitochondria function. Here, we found that apoE4 binds to ubiquinol cytochrome c reductase core protein 2 (UQCRC2) and cytochrome C1, both of which are components of mitochondrial respiratory complex III, and cytochrome c oxidase subunit 4 isoform 1 (COX IV 1), which is a component of complex IV, in Neuro-2a cells. Interestingly, these proteins associated with apoE4(1–272) more strongly than intact apoE4(1–299). Further analysis showed that in Neuro-2a cells expressing apoE4(1–272), the enzymatic activities of mitochondrial respiratory complexes III and IV were significantly lower than those in Neuro-2a cells expressing apoE4(1–299).

Conclusion: ApoE4(1–272) fragment expressed in Neuro2a cells is associated with mitochondrial proteins, UQCRC2 and cytochrome C1, which are component of respiratory complex III, and with COX IV 1, which is a member of complex IV. Overexpression of apoE4(1–272) fragment impairs activities of complex III and IV. These results suggest that the C-terminal-truncated fragment of apoE4 binds to mitochondrial complexes and affects their activities, and thereby leading to neurodegeneration.

Background

It has been shown that the prevalence of Alzheimer's disease (AD) is associated with the polymorphisms of genes related to cholesterol metabolism, including *apolipoprotein E (apoE)* [1-3], *ATP-binding cassette transporter A1 (ABCA1)* [4], and *CYP46*, the gene encoding cholesterol 24-hydroxylase [5,6]. Human apoE, a 34-kDa protein with 299 amino acids, has three major isoforms, apoE2, apoE3, and apoE4 [7-9]. It is well known that the possession of apoE4 allele is a major risk factor for Alzheimer's disease (AD) [1-3]. The apoE4 allele, which is found in 40–65% of cases of sporadic and familial AD, increases the occurrence and lowers the age of onset of the disease [3,10]. In the central nervous system, apoE is one of the major lipid acceptors [11,12] and interacts with ABCA1 [13] to remove cholesterol from cells and generate high-density lipoprotein (HDL) particles [14] in an apoE-isoform-specific manner [15-18]. Because apoE-HDL is the major cholesterol supplier in the brain and the supply of HDL-cholesterol is essential for synaptogenesis and neurite outgrowth in neurons [19,20], the apoE-isoform-dependent difference in HDL generation may result in the apoE-isoform-dependent difference in the maintenance of synaptic plasticity and the recovery of neurons from neuronal damage found in AD brains.

In addition to the role of apoE in modulating extracellular lipid transport, the isoform-dependent intracellular functions of apoE have also been reported. A previous report has shown that apoE3 recycling is associated with concomitant cholesterol efflux and thereby contributes to the formation of apoE-containing HDL, whereas apoE4 recycling is impaired and apoE4 accumulates within endosomal compartments, inducing an impaired cholesterol efflux [21], which may lead to the accumulation of cellular cholesterol and enhanced amyloid β-protein (Aβ) generation [22]. Another effect of reduced recycling of apoE4 is due to the tight binding of apoE4 to LDLR and LRP1 in the endosomal compartment [21], which in turn affects the interaction of the amyloid precursor protein (APP) and LRP1 that is crucial for the generation of Aβ [23,24]. Other lines of evidence have shown that apoE is cleaved by a protease to generate C-terminal-truncated fragments of apoE (residues 1–272) (apoE4(1–272)) in cultured neuronal cells, and the apoE(1–272) fragment is found in the brains of AD patients and transgenic mice expressing human apoE [25,26]. This proteolytic cleavage occurs in neurons, but not in astrocytes, and C-terminal-truncated fragments of apoE accumulated in an age-dependent manner in the brains of apoE4 mice and, to a significantly lesser extent, apoE3 mice [26]. These fragments, particularly apoE4(1–272), cause AD-like neurodegeneration and memory deficits in transgenic mice expressing apoE4(1–272) [27]. These lines of evidence suggest that the intraneuronal proteolytic processing of apoE could enhance the neuropathology and promote neurodegeneration in AD brains. It has been shown that the presence of a lipid-binding region of apoE (residues 244–272) is critical for apoE fragments to exert neurotoxicity in vivo [27]. Previous studies have shown that residues 267–299 are responsible for the tetramerization of apoE in solution, and the truncation of residues 273–299 in apoE4 gives rise to the monomeric form [28], and that these hydrophobic residues appear to be responsible for the neurotoxicity caused by the C-terminal-truncated apoE4 fragments [29]. In addition to the strong neurotoxicity caused by the apoE4(1–272) fragment, it has been shown that the apoE4(1–272) fragment accumulates in filamentous neurofibrillary tanglelike structures with phosphorylated tau in the cytosol or mitochondria, inducing mitochondrial dysfunction [25-27,29]. However, it still remains unclear how the apoE fragments are transported to the filamentous cytoplasmic structures or to mitochondria, and how they associate with mitochondria and induce mitochondrial dysfunction. To address these questions, we performed experiments to identify the proteins that associate with apoE4(1–272) or intact apoE4(1–299), and determine their functions. We identified three apoE4-binding proteins, all of which are components of mitochondria. We found that these proteins preferentially bind to apoE4(1–272) than to apoE4(1–299) and that the overexpression of apoE4(1–272) fragment decreases the enzymatic activities of mitochondrial respiratory complexes III and IV in cultured cells.

Results

Identification of apoE4-associated proteins

To identify molecules that specifically bind to apoE4, various fractions obtained from mouse brain were loaded onto a FLAG-apoE4(1–272) or FLAG-apoE4(1–299) affinity column. The proteins bound to these columns were eluted with an excess amount of FLAG peptide and the extracts were subjected to SDS-PAGE and silver staining. When each mouse brain fraction was loaded onto a FLAG-apoE4(1–272) or FLAG-apoE4(1–299) affinity column and eluted samples were subjected to SDS-PAGE, many protein bands were detected as candidate apoE4-associated proteins (Fig. 1). These bands were detected only when the mouse brain fractions and FLAG-apoE4 recombinant proteins coexisted.

To identify these proteins, the protein bands were subjected to LC-MS/MS analysis. As a result, we identified sixteen apoE4-associated proteins, which are shown in Table 1. These candidate proteins include the ATP synthase protein α and β subunits, which were previously reported [30]. Interestingly, ten among the candidate proteins are shown to be associated with mitochondria.

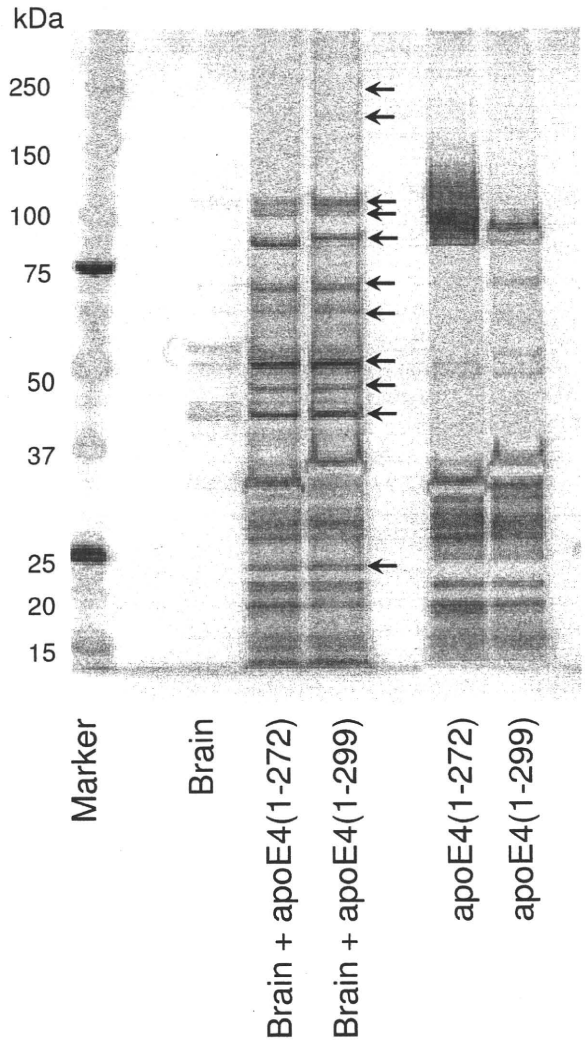

Figure 1
The proteins coimmunoprecipitated with apoE4 in the membrane extracts from mouse brain. Mouse brain membrane extracts were applied to the FLAG-apoE4(1–299) or FLAG-apoE4(1–272)-anti-FLAG M2-agarose affinity resin column and then eluted with the elution buffer. The eluant was dialyzed against the dialysis buffer, concentrated, and subjected to SDS-PAGE. The gels were stained with SilverQuest Silver Staining kit (Invitrogen). The protein bands (arrows), which were absent in the brain samples without apoE4s, and in the apoE4s samples without brain, were subjected to LC-MS/MS analysis.

Association of identified proteins with apoE4 in cultured cells

Next, we examined whether these proteins really associate with apoE in living cells. We cotransfected each candidate protein and FLAG-apoE4 into Neuro2a cells. Twenty-four hours following the transfection, the cells were harvested and treated with Triton X-100 solubilization buffer to obtain cell lysate as described in Materials and Methods. We carried out immunoprecipitation using these samples with an anti-FLAG antibody. The immunoprecipitate was then subjected to western blotting analysis using antibody specific for each protein or anti-HA antibody. This is because, in case we could not find antibodies specific for some candidate proteins, we could still generate HA-tagged proteins. Among the proteins identified by LC-MS/MS analysis, we found that three proteins, ubiquinol cytochrome c reductase core protein 2 (UQCRC2), cytochrome C1, and cytochrome *c* oxidase subunit 4 isoform 1 (COX IV 1) were associated with apoE4(1–299) and apoE4(1–272).

To examine whether mouse UQCRC2 is really associated with apoE proteins in cells, Neuro2a cells were cotransfected with mammalian expression plasmids encoding FLAG-apoE4(1–272) or FLAG-apoE4(1–299) and plasmids encoding mouse UQCRC2. Western blot analysis showed that the signal representing mouse UQCRC2 was clearly detected in the immunoprecipitate from the cells cotransfected with apoE4(1–272), while a very faint signal for UQCRC2 was detected in that from the cells cotransfected with apoE4(1–299). ApoE proteins were similarly immunoprecipitated in both samples (Fig. 2A). These results suggest that UQCRC2 prefers to associate with apoE4(1–272) than with apoE4(1–299).

To examine whether human UQCRC2 also associates with apoE4, we performed an experiment using human HA-tagged UQCRC2 expression vector. Similar to the results using mouse UQCRC2-transfected cells, the signals representing human HA-tagged UQCRC2 were clearly detected in the immunoprecipitate from the cells cotransfected with apoE4(1–272), while a very faint signal for HA-UQCRC2 was detected in that from the cells cotransfected with apoE4(1–299). Under these conditions, apoE4(1–272) and apoE4(1–299) proteins were similarly immunoprecipitated in both samples (Fig. 2B).

Next, we examined the association of human cytochrome C1 and apoE proteins using Neuro2a cells cotransfected with HA-tagged human cytochrome C1 expression vector and plasmids encoding FLAG-apoE4(1–272) or FLAG-apoE4(1–299). A strong signal for HA-tagged human cytochrome C1 was detected in the immunoprecipitate from the cell samples expressing apoE4(1–272), while a very faint signal for cytochrome C1 was detected in those transfected with apoE4(1–299) plasmid. ApoE4(1–272) and apoE4(1–299) proteins were similarly detected in both samples (Fig. 2C).

In addition, whether COX IV 1 is associated with apoE was determined. Human COX IV 1 was immunoprecipitated in the samples from apoE4(1–272)-expressing cells

Table 1: ApoE-associated proteins identified by LC-MS/MS analysis

Protein	Intracellular localization	Function
Solute carrier family 25 (mitochondrial carrier, Aralar) member 12	Mitochondria	Calcium-dependent mitochondrial aspartate and glutamate carrier
Ubiquinol cytochrome c reductase core protein 1	Mitochondria	Mitochondrial electron transport
* Ubiquinol cytochrome c reductase core protein 2 (UQCRC2)	Mitochondria	Mitochondrial electron transport
* Cytochrome C1	Mitochondria	Mitochondrial electron transport
Cytochrome oxidase subunit II	Mitochondria	Mitochondrial electron transport
* Cytochrome c oxidase subunit IV isoform 1 (COX IV1)	Mitochondria	Mitochondrial electron transport
ATP synthase, H+ transporting, mitochondrial F1 complex, α subunit, isoform 1	Mitochondria	ATP synthesis
ATP synthase, H+ transporting, mitochondrial F1 complex, β subunit	Mitochondria	ATP synthesis
ATP synthase, H+ transporting, mitochondrial F1 complex, δ subunit	Mitochondria	ATP synthesis
Methylenetetrahydrofolate dehydrogenase (NADP+ dependent)- 1 like	Mitochondria	Folic acid and derivative biosynthetic process
Syntaxin binding protein 1	Cytoplasm	Modulates exocytosis of dense-core granules
Nonmuscle myosin heavy chain	Cytoplasm	Actin filament-based movement
Tubulin, alpha 1A	Cytoplasm	Constituent of microtubules
RAB3A, member RAS oncogene family	Cytoplasm	Involved in exocytosis by regulating a late step in synaptic vesicle fusion.
Progesterone receptor membrane component 1	Plasma membrane	Receptor for progesterone
Cardiotrophin-like cytokine factor 1	Extracellular space	Cell surface receptor linked signal transduction

ApoE4-associated protein bands that were detected with SDS-PAGE were prepared and analyzed as described in the Methods. Asterisks (*) show the apoE-binding proteins identified and characterized in this study.

and a very faint signal for COX IV 1 was detected in the samples from apoE4(1–299)-expressing cells, whereas apoE4(1–272) and apoE4(1–299) proteins were similarly immunoprecipitated in both samples (Fig. 3). Interestingly, these proteins, UQCRC2, cytochrome C1, and COX IV 1, are associated more strongly with apoE4(1–272) than with apoE4(1–299). Concerning other proteins, we carried out similar experiments; however, no association of these proteins with apoE4(1–272) and apoE4(1–299) was found in cultured cells (data not shown).

The levels of apoE4 in mitochondrion-rich fraction isolated from ApoE4(1–272)- or ApoE4(1–299)-expressing cells

The results indicate that apoE4(1–272) binds to mitochondrial proteins; therefore, we next determined whether the levels of apoE4(1–272) and apoE4(1–299) are also associated with the mitochondria. We, thus, determined the levels of apoE4(1–272) and apoE4(1–299) in mitochondrion-rich fractions isolated from Neuro2a cells transfected with apoE4(1–272) or apoE4(1–299). The level of apoE4(1–272) in the pellet, a mitochondrion-rich fraction, was greater than that of apoE4(1–299) (Fig. 4). VDAC, a mitochondrion marker, was recovered in the pellet fraction (Fig. 4).

Effect of apoE4(1–272) overexpression on activities of mitochondrial respiratory complexes

It is known that UQCRC2 and cytochrome C1 are subunits of mitochondrial respiratory complex III and COX IV 1 is a subunit of mitochondrial respiratory complex IV. It

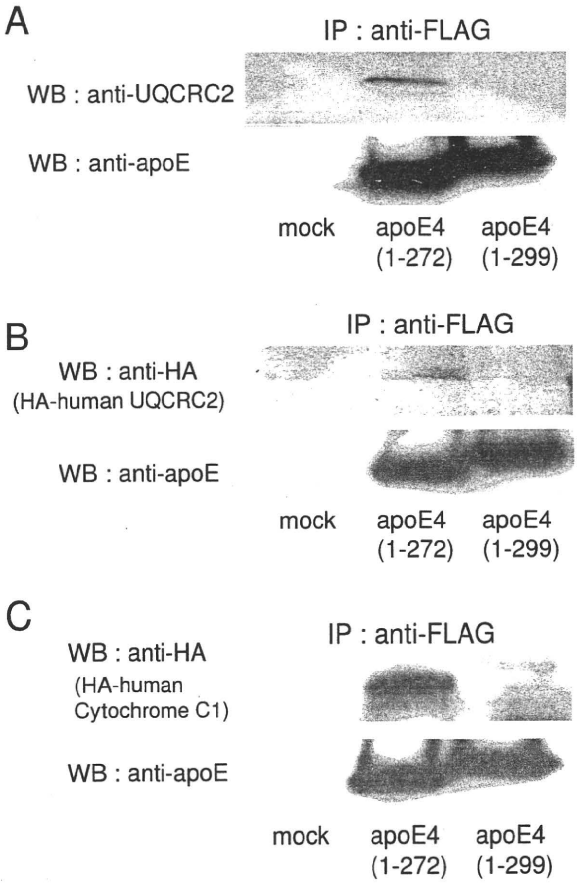

Figure 2
ApoE4 interacts with the subunits of mitochondrial respiratory complex III in Neuro2a cells. Neuro2a cells were cotransfected with mammalian expression plasmids encoding FLAG-apoE4(1–272) or FLAG-apoE4(1–299) and plasmids encoding mouse UQCRC2, human HA-UQCRC2, or human HA-cytochrome C1, all of which are candidate proteins suggested to be associated with apoE4 (Table 1). Twenty-four hours following the transfection, the cells were harvested and treated with 500 μl of Triton X-100 solubilization buffer to obtain cell lysate. The cell lysate was then incubated with anti-FLAG M2-agarose affinity resin, and the protein binding to the affinity column was eluted using FLAG peptide, and the eluted protein was then analyzed by western blotting with anti-UQCRC2 (mouse UQCRC2) antibody (A), anti-HA antibody (human UQCRC2) (B), or anti-HA antibody (human cytochrome C1) (C).

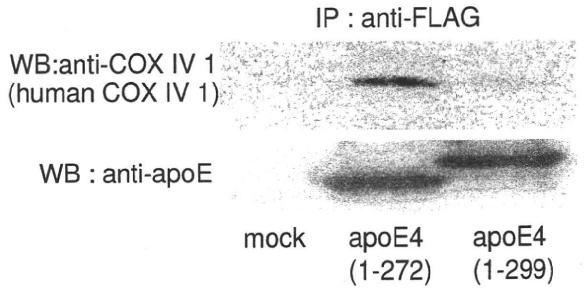

Figure 3
ApoE4 interacts with the subunits of mitochondrial respiratory complex IV in Neuro2a cells. Neuro2a cells were co-transfected with FLAG-apoE4 (1–272 or 1–299) plasmids and mammalian expression plasmids encoding the candidate apoE4-associated proteins. The cells were treated with 500 μl of Triton X-100 solubilization buffer and the cell lysate was incubated with anti-FLAG M2-agarose affinity resin. The immunoprecipitates were then analyzed by western blotting with an anti-COX IV 1 antibody (human COX IV 1).

was reported that apoE4(1–272) induces mitochondrial dysfunction [25-27,29]. Because these proteins are associated more strongly with apoE4(1–272) than with apoE4(1–299), we investigated whether the enzymatic activities of mitochondrial respiratory complexes III and IV change, when apoE4(1–272) is overexpressed in cultured cells. Complex III activity was expressed as the difference in the reduction of cytochrome *c* with or without antimycin A and myxothiazol, both of which are complex III inhibitors. Expectedly, the complex III activity of apoE4(1–272)-overexpressing Neuro2a cells was lower than that of apoE4(1–299)-overexpressing cells (Fig. 5A). Because apoE4(1–272) associates with UQCRC2 and cytochrome C1, there was a possibility that the decrease in complex III activity in Neuro2a cells expressing apoE4(1–272) was due to the interaction between apoE4 and complex III. Complex IV activity was expressed as the difference in the oxidation of ferrocytochrome C with or without KCN and Na_3N, both of which are complex IV inhibitors. The complex IV activity of apoE4(1–272)-overexpressing cells was significantly lower than that of apoE4(1–299)-overexpressing cells (Fig. 5B). The levels of the mitochondrial proteins UQCRC2 and cytochrome C1 in apoE4(1–272)- and apoE4(1–299)-overexpressing cells were similar, as demonstrated by western blot analysis using anti-UQCRC2 and anti-cytochrome C1 antibodies (Fig. 5C).

Effects of overexpression of apoE4(1–272) and apoE4(1–299) on ATP synthase activity and mitochondrial membrane potential

Because apoE4(1–272) decreases the activities of mitochondrial complexes III and IV, we next examined whether the overexpression of apoE4(1–272) also affects ATP synthase activity and mitochondrial membrane potential. Unexpectedly, apoE4(1–272) and apoE4(1–299) showed no effect on ATP synthase activity (Fig. 6A). We further examined the effect of the overexpression of

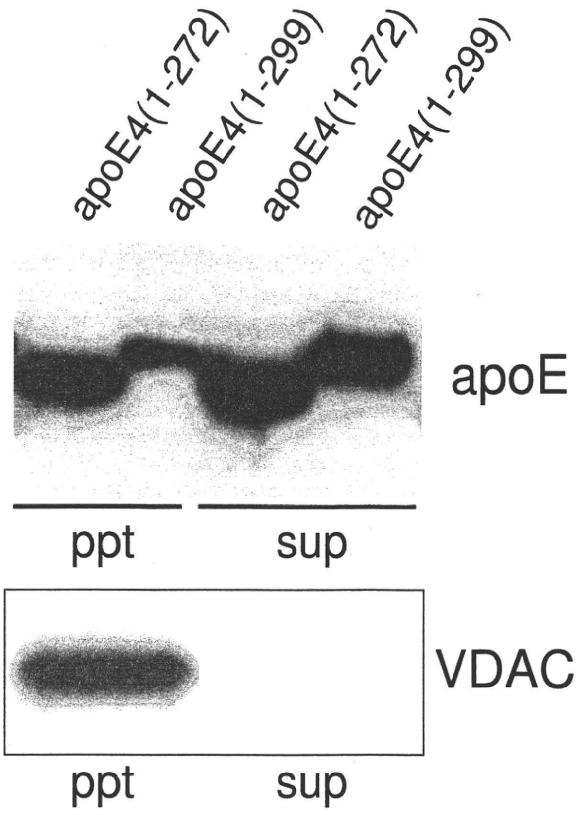

Figure 4
The level of apoE4(1–272) recovered from the mitochondrion-rich fraction is greater than that of apoE4(1–299). Neuro2a cells transfected with ApoE4(1–272) and ApoE4(1–299) plasmids were harvested and homogenized with a homogenizing buffer (10 mM Tris-HCl, pH 7.4, 1 mM EDTA, 0.25 M sucrose), and the resulting homogenate was centrifuged at 1,000 *g* for 10 min at 4°C. The resulting supernatant was further centrifuged at 8,000 *g* for 20 min at 4°C. The resulting precipitate (ppt) was used as the mitochondrion-rich fraction. Equal amounts of proteins from the ppt and supernatant (sup) fractions were analyzed by western blot analysis using the anti-apoE antibody, AB946, and the anti-VDAC antibody. VDAC was used as the mitochondrion marker.

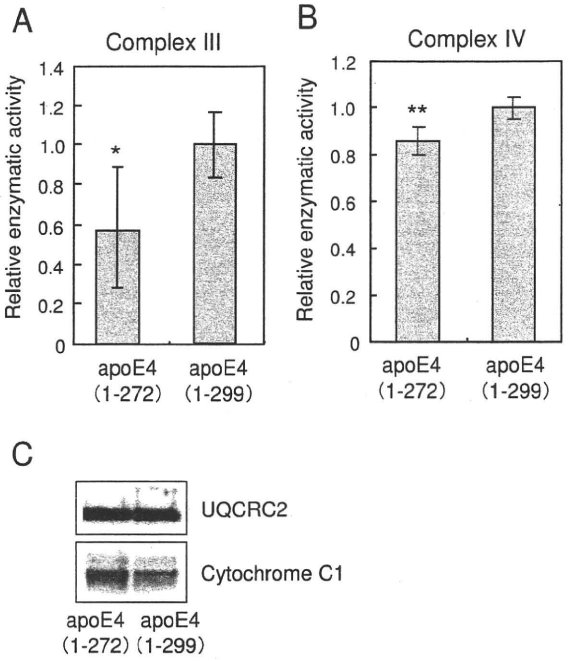

Figure 5
Overexpression of apoE4(1–272) results in the decreased level of complex III and IV activities. Enzymatic assays of respiratory chain complexes III (A) and IV (B) from Neuro2a cells overexpressing FLAG-apoE4(1–272 or 1–299) were determined as described in the Methods. The mitochondria levels in apoE4(1–272)- and apoE4(1–299)-overexpressing cells were determined by western blot analysis using the anti-UQCRC2 and the anti-cytochrome C1 antibodies (C). Data are the mean ± SEM of nine independent experiments. * $P < 0.005$, ** $P < 0.0005$ (t-distribution test).

apoE4(1–272) and apoE4(1–299) on mitochondrial membrane potential. Neuro2a cells transfected with these apoE4 species were stained with JC-1, a fluorescent dye that has been shown to be a reliable indicator of mitochondrial membrane potential changes in intact cells. After three hours of treatment of Neuro2a cells with 1 μM valinomycin, a K^+ ionophore that disrupts the transmembrane electrical gradient, the intensity of red fluorescence (FL2) markedly decreased, whereas that of green fluorescence (FL1) slightly increased, as demonstrated by JC-1 staining (Fig. 6B), indicating the dissipation of mitochondrial membrane potential. On the other hand, there were no significant differences in FL1 and FL2 intensities among Neuro2a cells transfected with mock, apoE4(1–272) and apoE4(1–299) (Figs. 6B, C, and 6D), indicating that the overexpression of apoE4(1–272) and apoE4(1–299) has no effect on mitochondrial membrane potential.

Discussion

Here, we show the molecules associated with apoE protein. Among the molecules identified, we show for the first time that apoE4, particularly C-terminal cleaved apoE4(1–272), binds to UQCRC2 cytochrome C1 and COX IV 1. Although apoE(1–272) has been shown to be translocated to mitochondria, it still remains unclear how the apoE fragments associate with mitochondria and induce mitochondrial dysfunction. The present study has shown that apoE4(1–272) binds to UQCRC2 cytochrome C1, a component of complex III, and COX IV 1, a component of complex IV, and that overexpression of apoE(1–

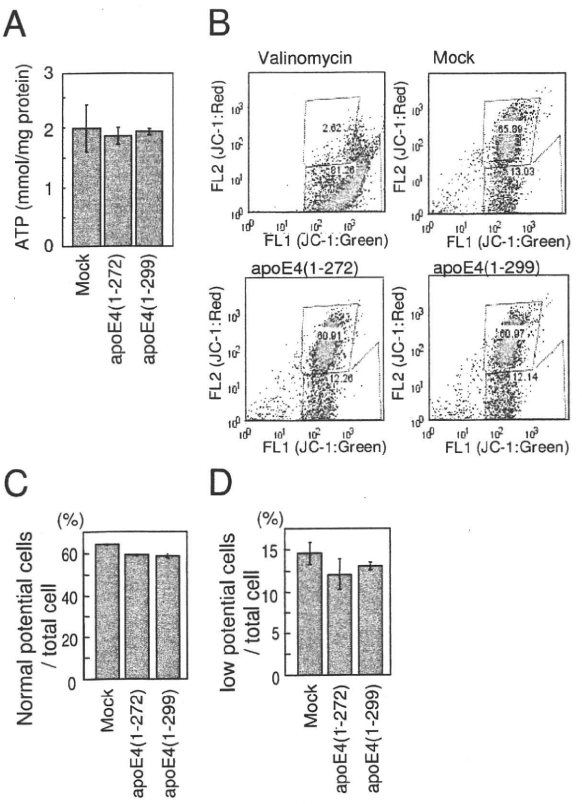

Figure 6
Effects of overexpression of apoE4(1–272) and apoE4(1–299) on ATP synthase activity and mitochondrial membrane potential. The ATP synthase activity in Neuro2a cells transfected with the ApoE4(1–272) and ApoE4(1–299) plasmids were determined (A) as described in the Methods. The data are the mean ± SEM of three experiments. (B) Flow cytometry plots were used to determine the ratio of cells having normal and low mitochondrial membrane potentials, which were demonstrated by staining with the JC-1 dye. The distribution of the cells sorted by FACS was analyzed, and the ratios of the number of cells showing normal membrane potential (C) and low membrane potential (D) to total cell number were calculated.

272) fragment in Neuro2a cells results in decreases in the levels of complex III and complex IV activities compared with those in cells overexpressing intact apoE4. These results suggest that the apoE4(1–272) fragment binds to UQCRC2 cytochrome C1 and COX IV 1, thereby inhibiting complex III and complex IV activities, respectively. The candidate molecules, which may associate with apoE to transport apoE to mitochondria, were not identified in our present analysis (Table 1). This should be addressed in a future study.

Another finding in the present study is that UQCRC2 cytochrome C1 and COX IV 1 are associated more strongly with ApoE4(1–272) than with intact apoE4(1–299) (Figs. 2, 3). There are at least two possible explanations for this result. One explanation is that apoE4(1–272) is structurally different from apoE4(1–299), resulting in the difference in hydrophobicity or binding affinity to other proteins. It has been shown that the C-terminus of apoE (residues 253–289) participates in hydrophobic interactions that stabilize the tetramer [28], and that these hydrophobic residues are suggested to be responsible for inducing neurotoxicity caused by the C-terminal-truncated apoE4 [29]. In addition, a recent study has shown that apoE4 lacking a hydrophobic C-terminal α-helical segment (residues 273–299) found in brain leads to a less organized C-terminal structure that is available for interaction with cell membranes and other proteins such as Aβ [31]. Another explanation is that more apoE(1–272) is translocated to mitochondria than intact apoE(1–299), because the silver staining shows that the intensities of the bands representing apoE-associated proteins were not different between the samples containing apoE4(1–272) and apoE4(1–299) (Fig. 1), whereas the level of apoE4(1–272) was greater than that of apoE4(1–299) in the mitochondrion-rich fraction of Neuro2a cells expressing apoE4(1–272) and apoE4(1–299) (Fig. 4). Although the precise mechanism underlying this difference is yet unknown, it is possible that the truncation of residues 273–299 in apoE4 leads to the reorganization of the C-terminal domain, with a lipid-binding region being less organized and available for hydrophobic interaction including Aβ [31-33].

Regarding the mitochondrial dysfunction in Alzheimer disease, there are previous reports showing that the overexpression of amyloid precursor protein increases the level of Aβ in mitochondria [34], and that mitochondrial complex III and IV activities are decreased in Tg2576 mouse brains [34]. In addition, the complex IV activity was shown to decrease in the brain of AD patients [35-39]. Moreover, it has been shown that the apoE(1–272) fragment is generated at a greater level from apoE4 than apoE3, and the overexpression of apoE isoform-dependently affects mitochondrial function [27]. These lines of evidence together with our present study suggest that the greater level of apoE4(1–272) fragment generated from apoE4 may be associated with Aβ that is transported to mitochondria and binds to UQCRC2 cytochrome C1 and COX IV 1, and causes mitochondrial dysfunction.

Complexes III and IV are related to ATP synthesis and the maintenance of mitochondrial membrane potential, which are critical for cell survival. Thus, we examined the

effect of the transient expressions of apoE4(1–272) and apoE4(1–299) on ATP synthesis and membrane potential in Neuro2a cells. Unexpectedly, there was no difference between apoE4(1–272)- and apoE4(1–299)-transfected cells in terms of the levels of ATP synthesis or membrane potential (Fig. 6). However, when we tried to generate the Neuro2a cells, in which apoE4(1–272) is stably expressed, all the cells were dead within 2 weeks after the transfection, whereas apoE4(1–299)-expressing cells remained alive. These results suggest that apoE4(1–272) may have neurotoxicity as previously reported [29], although the level of toxicity is low. This issue remains to be addressed in further studies.

One may consider that apoE is synthesized as a secretory protein; however, how apoE enters the cytosol remains unclear and controversial. Previous studies have shown that apoE escapes the secretory or endosomal internalization pathway, and enters the cytosol of neuronal cells [25,29,40] and non-neuronal cells [41], whereas another study has failed to show this [42]. Therefore, the physiological relevance of the three mitochondrial proteins that we have identified in this study, which are associated with apoE, remains to be confirmed under physiological conditions.

It is well known that apoE4 is a strong risk factor for AD development, and the regulation of apoE4 function may be a therapeutic target for AD. Our findings indicate that if we could modulate the generation of apoE4(1–272) and/or modulate its translocation to mitochondria, the apoE4-associated induction of neurodegeneration could be prevented or attenuated. Because it has been shown that the C-terminus of the apoE-cleaving enzyme is a neuron-specific, chymotrypsin-like serine protease [25-27], the characterization and modulation of this enzyme activity would be a therapeutic target for AD.

Conclusion

We identified intracellular apoE-binding molecules and determined their functions in modulating mitochondria function. The ApoE-binding molecules we found are ubiquinol cytochrome *c* reductase core protein 2 (UQCRC2), cytochrome C1, and cytochrome *c* oxidase subunit 4 isoform 1 (COX IV 1). The UQCRC2 and cytochrome C1 are components of mitochondrial respiratory complex III, and COX IV 1 is a component of complex IV. Interestingly, these proteins associated with apoE4(1–272) more strongly than intact apoE4 (1–299). When apoE4(1–272) expression level increased in Neuro2a cells, the enzymatic activities of mitochondrial respiratory complexes III and IV were significantly lower than those in Neuro-2a cells expressing apoE4(1–299). These results suggest that the C-terminal-truncated fragment of apoE4(1–272) bind to mitochondrial complexes and affects their activities.

Methods

Preparation of mouse brain membrane extracts and cytosolic fraction

Brains obtained from C57BL6 male mice were homogenized with a homogenizing buffer (10 mM Tris-HCl, pH 7.4 1 mM EDTA 0.25 M sucrose), and the homogenate was centrifuged at 1,000 *g* for 10 min at 4°C. The supernatant was recentrifuged at 10,000 *g* for 20 min at 4°C, and the resulting precipitate was suspended in a homogenizing buffer. The supernatant was recentrifuged at 100,000 *g* for 1 min at 4°C, and the resulting precipitate was suspended in a homogenizing buffer. The supernatant was used as the cytosolic fraction. The proteins in the 10,000 *g* and 100,000 *g* pellet fraction were extracted with homogenizing buffer containing 1 M KCl. The resulting pellet was solubilized with 2% Triton X-100 for 1 h at 4°C and then centrifuged at 100,000 *g* of 1 h at 4°C. The supernatants were used as 10,000 *g* or 100,000 *g* membrane extracts.

FLAG fusion proteins

Recombinant FLAG-apoE4 fusion proteins encoding WT (1–299) or C-terminal truncated apoE4 (1–272) were prepared and purified as follows. PCR products encoding apoE4 (1–272) and apoE4 (1–299) were subcloned into pFLAG-MAC expression vector (Sigma). These plasmids were transformed into the BL21 strain of *Escherichia coli* and induced with isopropyl-1-thio-b-$_D$-galactopyranoside to produce FLAG fusion proteins. The bacteria were suspended in PBS, and vigorous sonication was performed before centrifugation at 10,000 *g* for 20 min. The resulting supernatants were applied to anti-FLAG M2-agarose affinity resin column (Sigma) and then eluted with an elution buffer (TBS containing 100 μg/ml FLAG peptide (Sigma)). Purified FLAG fusion proteins were dialyzed against TBS.

FLAG-ApoE4 affinity chromatography and LC-MS/MS analysis

Recombinant FLAG-apoE4(1–299) or FLAG-apoE4(1–272) fusion protein coupled to anti-FLAG M2-agarose affinity resin was used to identify affinity-purified apoE4-binding proteins. The fractionated mouse brain samples were applied to the FLAG-apoE4(1–299)- and FLAG-apoE4(1–272)-anti-FLAG M2-agarose affinity resin column. The proteins bound to the resin column were then eluted with the elution buffer. The eluted proteins were dialyzed against the dialysis buffer, concentrated, and subjected to SDS-PAGE. The gels were stained with Silver-Quest Silver Staining kit (Invitrogen). The proteins specifically associated with apoEs demonstrated as silver-

stained bands were cut out, digested with trypsin, and subjected to LC-MS/MS analysis.

LC-MS/MS analysis

The proteins in the silver-stained bands were reduced with 10 mM dithiothreitol at room temperature for 2 h and alkylated with 40 mM iodoacetamide in the dark at room temperature for 30 min. Each sample was digested with trypsin (4 μg/ml; Trypsin Gold, Promega) in 40 mM NH_4HCO_3/10%ACN at 37°C overnight. The extracted peptides were then separated via nano liquid chromatography (LC) (Paradigm MS4, Michrom BioResources, Inc., Auburn, CA) using a Magic C18 column (0.2 × 50 mm; Michrom BioResources, Inc.; Auburn, CA). The LC eluent was analyzed using an LCQ Advantage MAX mass spectrometer (Thermo Fisher Scientific) equipped with an ion-spray source. All MS/MS spectra were searched by SEQUEST algorithm from BioWorks software (Thermo Fisher Scientific).

Cells

Neuro2a cells were grown in DMEM medium, supplemented with 10% FBS, 50 units/ml penicillin, 50 mg/ml streptomycin, and 2 mM glutamine at 37°C in a humidified 5% CO_2 95% air incubator.

Transfection of plasmids into cells and co-immunopricipitation

PCR products encoding apoE4 (1–272) and apoE4 (1–299) were subcloned into pFLAG-CMV-2 expression vector (Sigma). Neuro2a cells were co-transfected with FLAG-apoE4 (1–272 or 1–299) plasmids and mammalian expression plasmids coding the candidate of apoE4 associating proteins (Toyobo, Japan) using Lipofectamine 2000 (Invitrogen, CA, USA). As necessary, mammalian expression plasmids coding the candidate apoE4-associated proteins were fused with HA-tag of their C-terminus using KOD-PLUS Mutagenesis Kit (Toyobo). The plasmids were transfected to Neuro2a cells as follows. Neuro2a cells were plated on a 6-cm plate at a cell density of 1.5×10^6 and cultured in the culture medium described above. The next day, the ells were transfected with the plasmid employing Lipofectamine 2000 reagent. On culture day 3, the cells were lysed with 500 μl of Triton X-100 solubilization buffer (10 mM Tris-HCl (pH 7.4), 150 mM NaCl, 1 mM EDTA, 10 mg/ml leupeptin, 1 mM PMSF, 0.5% Triton X-100). The cell lysate was incubated with anti-FLAG M2-agarose affinity resin. After an overnight incubation at 4°C, the beads were washed three times with Triton X-100 solubilization buffer and then eluted with the elution buffer (PBS containing FLAG peptide at a concentration of 100 μg/ml). The immunoprecipitates were then analyzed by western blotting with anti-HA monoclonal antibody (Sigma), anti-UQCRC2 monoclonal antibody (Abcam), and anti-COX IV 1 monoclonal antibody (Cell Signaling).

Enzymatic analysis of complexes III and IV

Mitochondria isolated from homogenates of Neuro2a cells transfected with ApoE4 (1–299 or 1–272) were used for enzymatic analysis.

(a) Complex III (Ubiquinol cytochrome c reductase)

The oxidation of ubiquinol$_2$ by complex III was determined using cytochrome *c* (III) as an electron acceptor. The assay was carried out in an assay medium (25 mM potassium phosphate buffer (pH 8.0), 1 mM EDTA, 1 mM KCN, 3 mM Na_3N) supplemented with 20 μM cytochrome *c* (III), and 20 μM ubiquinol$_2$. The reaction was started with 5 μg of mitochondrial protein and the enzyme activity was measured at 550 nm. The activity of complex III is estimated to be the difference in the reduction of cytochrome *c* with and without 10 μg/ml antimycin A and 10 μg/ml myxothiazol.

(b) Complex IV (Cytochrome c Oxidase)

The enzyme activity of cytochrome *c* oxidase (complex IV) was determined using Mitochondria Activity Assay kit (BioChain Institute, U.S.A.) and performed following the manufacture's procedure. Complex IV activity was measured as the oxidation of ferrocytochrome *c* by cytochrome *c* oxidase at 550 nm. Complex IV activity is expressed as the difference in the oxidation of ferrocytochrome C with or without KCN and Na_3N as complex IV inhibitor.

ATP synthase activity assay

Neuro2a cells transfected with apoE4(1–272) and apoE4(1–299) plasmids were harvested and homogenized with a homogenizing buffer (10 mM Tris-HCl, pH 7.4, 1 mM EDTA, 0.25 M sucrose), and the homogenate was centrifuged at 1,000 *g* for 10 min at 4°C. The resulting supernatant was further centrifuged at 10,000 × g for 20 min at 4°C, and the resulting pellet (ppt) fractions were obtained. The ppt fractions were resuspended in 100 μl of assay buffer (1 mM ADP and 5 mM sodium succinate) and incubated for 5 min at 37°C. 100 mM Tris-HCl buffer (pH 7.6) containing 4 mM EDTA was added and the fractions were further incubated for 2 min at 100°C. Then the fractions were plated on ice and ATP level in each fraction was determined using an ATP bioluminescence assay kit CLS II (Roche Diagnosis GmbH, Mannheim, Germany).

Analysis of mitochondrial membrane potential (mt)

ApoE4(1–272 or 1–299)-transfected Neuro2a cells were stained with 2 μM JC-1 (Molecular Probes, Eugene, OR) at 37°C for 20 min. Then, the cells were analyzed using a flow cytometer FACSCalibur (Becton Dickinson, Franklin Lakes, NJ) with FlowJo software (Tree Star Inc., Ashland, OR).

Statistical analysis

StatView computer software (Windows) was used for statistical analysis. Statistical significance of differences

between samples was evaluated by multiple pairwise comparisons among the sets of data using ANOVA and the Bonferoni t-test.

Competing interests

The authors declare that they have no competing interests.

Authors' contributions

TN carried out major part of the experiments. AW carried out TOF-MS/MS analysis and identified molecules associated with apoE. TF generated plasmid containing intact apoE3 and apoE4 cDNA. TH prepared cultured cells. MM designed this study and was involved in the interpretation of the results and in drafting the manuscript.

Acknowledgements

This work was supported by Grant-in-Aid for Scientific Research on Priority Areas-Research on Pathomechanisms of Brain Disorders-from the Ministry of Education, Culture, Sports, Science and Technology of Japan, a grant from the Program for Promotion of Fundamental Studies in Health Sciences of the National Institute of Biomedical Innovation (NIBRO), and a rant from the Ministry of Health, Labor and Welfare of Japan (Comprehensive Research on Aging and Health Grant H20-007).

References

1. Strittmatter WJ, Saunders AM, Schmechel D, Pericak-Vance M, Enghild J, Salvesen GS, Roses AD: **Apolipoprotein E: high-avidity binding to beta-amyloid and increased frequency of type 4 allele in late-onset familial Alzheimer disease.** *Proc Natl Acad Sci USA* 1993, **90:**1977-1981.
2. Roses AD: **Apolipoprotein E affects the rate of Alzheimer disease expression: beta-amyloid burden is a secondary consequence dependent on APOE genotype and duration of disease.** *J Neuropathol Exp Neurol* 1994, **53:**429-37.
3. Corder EH, Saunders AM, Strittmatter WJ, Schmechel DE, Gaskell PC, Small GW, Roses AD, Haines JL, Pericak-Vance MA: **Gene dose of apolipoprotein E type 4 allele and the risk of Alzheimer's disease in late onset families.** *Science* 1993, **261:**921-923.
4. Wollmer MA, Streffer JR, Lutjohann D, Tsolaki M, Iakovidou V, Hegi T, Pasch T, Jung HH, Bergmann K, Nitsch RM, Hock C, Papassotiropoulos A: **ABCA1 modulates CSF cholesterol levels and influences the age at onset of Alzheimer's disease.** *Neurobiol Aging* 2003, **24:**421-426.
5. Kolsch H, Lutjohann D, Ludwig M, Schulte A, Ptok U, Jessen F, von Bergmann K, Rao ML, Maier W, Heun R: **Polymorphism in the cholesterol 24S-hydroxylase gene is associated with Alzheimer's disease.** *Mol Psychiatry* 2002, **7:**899-902.
6. Papassotiropoulos A, Streffer JR, Tsolaki M, Schmid S, Thal D, Nicosia F, Iakovidou V, Maddalena A, Lutjohann D, Ghebremedhin E, Hegi T, Pasch T, Traxler M, Bruhl A, Benussi L, Binetti G, Braak H, Nitsch RM, Hock C: **Increased brain beta-amyloid load, phosphorylated tau, and risk of Alzheimer disease associated with an intronic CYP46 polymorphism.** *Arch Neurol* 2003, **60:**29-35.
7. Mahley RW: **Apolipoprotein E: cholesterol transport protein with expanding role in cell biology.** *Science* 1988, **240:**622-630.
8. Mahley RW, Huang Y: **Apolipoprotein E: from atherosclerosis to Alzheimer's disease and beyond.** *Curr Opin Lipidol* 1999, **10:**207-17.
9. Mahley RW, Rall SC Jr: **Apolipoprotein E: far more than a lipid transport protein.** *Annu Rev Genomics Hum Genet* 2000, **1:**507-37.
10. Farrer LA, Cupples LA, Haines JL, Hyman B, Kukull WA, Mayeux R, Myers RH, Pericak-Vance MA, Risch N, van Duijn CM: **Effects of age, sex, and ethnicity on the association between apolipoprotein E genotype and Alzheimer disease. A meta-analysis. APOE and Alzheimer Disease Meta Analysis Consortium.** *JAMA* 1997, **278:**1349-1356.
11. Roheim PS, Carey M, Forte T, Vega GL: **Apolipoproteins in human cerebrospinal fluid.** *Proc Natl Acad Sci USA* 1979, **76:**4646-4649.
12. Pitas RE, Boyles JK, Lee SH, Hui D, Weisgraber KH: **Lipoproteins and their receptors in the central nervous system. Characterization of the lipoproteins in cerebrospinal fluid and identification of apolipoprotein B, E(LDL) receptors in the brain.** *J Biol Chem* 1987, **262:**14352-14360.
13. Krimbou L, Denis M, Haidar B, Carrier M, Marcil M, Genest J: **Molecular interactions between apolipoprotein E and the ATP-binding cassette transporter A1 (ABCA1): Impact on ApoE lipidation.** *J Lipid Res* 2004, **45:**839-848.
14. Ito J, Zhang LY, Asai M, Yokoyama S: **Differential generation of high-density lipoprotein by endogenous and exogenous apolipoproteins in cultured fetal rat astrocytes.** *J Neurochem* 1999, **72:**2362-2369.
15. Michikawa M, Fan QW, Isobe I, Yanagisawa K: **Apolipoprotein E exhibits isoform-specific promotion of lipid efflux from astrocytes and neurons in culture.** *J Neurochem* 2000, **74:**1008-1016.
16. Gong JS, Kobayashi M, Hayashi H, Zou K, Sawamura N, Fujita SC, Yanagisawa K, Michikawa M: **Apolipoprotein E (ApoE) isoform-dependent lipid release from astrocytes prepared from human ApoE3 and ApoE4 knock-in mice.** *J Biol Chem* 2002, **277:**29919-29926.
17. Xu Q, Brecht WJ, Weisgraber KH, Mahley RW, Huang Y: **Apolipoprotein E4 domain interaction occurs in living neuronal cells as determined by fluorescence resonance energy transfer.** *J Biol Chem* 2004, **24:**25511-25516.
18. Gong JS, Morita SY, Kobayashi M, Handa T, Fujita SC, Yanagisawa K, Michikawa M: **Novel action of apolipoprotein E (ApoE): ApoE isoform specifically inhibits lipid-particle-mediated cholesterol release from neurons.** *Mol Neurodegener* 2007, **2:**9.
19. Mauch DH, Nagler K, Schumacher S, Goritz C, Muller EC, Otto A, Pfrieger FW: **CNS synaptogenesis promoted by glia-derived cholesterol.** *Science* 2001, **294:**1354-7.
20. Hayashi H, Campenot RB, Vance DE, Vance JE: **Glial lipoproteins stimulate axon growth of central nervous system neurons in compartmented cultures.** *J Biol Chem* 2004, **279:**14009-15.
21. Heeren J, Grewal T, Laatsch A, Becker N, Rinninger F, Rye K-A, Beisiegel U: **Impaired Recycling of Apolipoprotein E4 Is Associated with Intracellular Cholesterol Accumulation.** *J Biol Chem* 2004, **279:**55483-55492.
22. Fassbender K, Simons M, Bergmann C, Stroick M, Lutjohann D, Keller P, Runz H, Kuhl S, Bertsch T, von Bergmann K, Hennerici M, Beyreuther K, Hartmann T: **Simvastatin strongly reduces levels of Alzheimer's disease beta-amyloid peptides Abeta 42 and Abeta 40 in vitro and in vivo.** *Proc Natl Acad Sci USA* 2001, **98:**5856-61.
23. Cole SL, Vassar R: **The Alzheimer's disease beta-secretase enzyme, BACE1.** *Mol Neurodegener* 2007, **2:**22.
24. Cam JA, Zerbinatti CV, Li Y, Bu G: **Rapid endocytosis of the low density lipoprotein receptor-related protein modulates cell surface distribution and processing of the beta-amyloid precursor protein.** *J Biol Chem* 2005, **280:**15464-70.
25. Huang Y, Liu XQ, Wyss-Coray T, Brecht WJ, Sanan DA, Mahley RW: **Apolipoprotein E fragments present in Alzheimer's disease brains induce neurofibrillary tangle-like intracellular inclusions in neurons.** *Proc Natl Acad Sci USA* 2001, **98:**8838-43.
26. Brecht WJ, Harris FM, Chang S, Tesseur I, Yu GQ, Xu Q, Dee Fish J, Wyss-Coray T, Buttini M, Mucke L, Mahley RW, Huang Y: **Neuron-specific apolipoprotein e4 proteolysis is associated with increased tau phosphorylation in brains of transgenic mice.** *J Neurosci* 2004, **24:**2527-34.
27. Harris FM, Brecht WJ, Xu Q, Tesseur I, Kekonius L, Wyss-Coray T, Fish JD, Masliah E, Hopkins PC, Scearce-Levie K, Weisgraber KH, Mucke L, Mahley RW, Huang Y: **Carboxyl-terminal-truncated apolipoprotein E4 causes Alzheimer's disease-like neurodegeneration and behavioral deficits in transgenic mice.** *Proc Natl Acad Sci USA* 2003, **100:**10966-71.
28. Fan D, Li Q, Korando L, Jerome WG, Wang J: **A monomeric human apolipoprotein E carboxyl-terminal domain.** *Biochemistry* 2004, **43:**5055-64.
29. Chang S, Ma Tr, Miranda RD, Balestra ME, Mahley RW, Huang Y: **Lipid- and receptor-binding regions of apolipoprotein E4**